Article

Herbicidal Activity of Beflubutamid Analogues as PDS Inhibitors and SAR Analysis and Degradation Dynamics in Wheat

Meng Zhang, Hui Cai, Dan Ling, Chen Pang, Jinming Chang, Zhichao Jin,* and Yonggui Robin Chi*

Cite This: https://doi.org/10.1021/acs.jafc.3c04733

Read Online

ACCESS | 📊 Metrics & More | 📖 Article Recommendations | 🆂🅸 Supporting Information

ABSTRACT: In this work, a series of beflubutamid (BF) analogues' postemergent herbicidal activity was evaluated, and the structure−activity relationship (SAR) was discussed. At a dosage of 300 g ai/ha, compounds (*Rac*)-**6h** and (*Rac*)-**6q** showed excellent herbicidal activity against *Amaranthus retroflexus*, *Abutilon theophrasti*, and *Medicago sativa*, with inhibition rates of 90, 100, and 80% and 100, 100, and 100%, respectively, comparable to that of commercial herbicide BF, which showed inhibition rates of 90, 100, and 100%, respectively. Notably, at dosages of 150 and 300 g ai/ha, the chiral compounds (*S*)-**6h** and (*S*)-**6q** exhibited higher herbicidal activities than their racemates. Molecular docking results indicated that compounds (*S*)-BF and (*S*)-**6h** have stronger binding affinities with *Oryza sativa* phytoene desaturase (*Os*PDS), resulting in a higher herbicidal activity. Additionally, the degradation dynamics half-life of (*S*)-BF in wheat was determined to be 77.02 h. Consequently, compounds (*S*)-**6h** and (*S*)-**6q** are promising lead candidates for the development of highly effective herbicides.

KEYWORDS: *PDS, herbicidal activity, structure−activity relationship, digestive dynamics, wheat*

INTRODUCTION

According to the National Bureau of Statistics of China, the grain sown area in China reached 118.3 million ha with a total production of 686.5 million tons in 2022.[1] But weed infestation poses a significant threat to crop yields, as they compete with crops for nutrients, light, and water, leading to yield reductions of more than one-third. Effective weed control through herbicide application is crucial to increasing crop productivity.[2−4] However, prolonged and extensive use of single herbicides, such as acetyi coa-carboxylase (ACCase) and acetolactate synthase (ALS) inhibitors, has resulted in severe weed resistance.[5] This necessitates higher herbicide dosages to eradicate resistant weeds, resulting in significant environmental pollution.[6−8] Therefore, to overcome weed resistance, there is an urgent need to develop novel herbicides with high activity, high selectivity, and environmental friendliness.[9]

In recent years, the stereochemistry of chiral pesticides has garnered increasing attention among researchers. Stereoisomers of pesticides exhibit distinct differences in bioactivity and environmental toxicity. For example, BF is a chiral herbicide composed of a pair of corresponding isomers. The *S* configuration of BF exhibits herbicidal activity that is 1000 times higher than that of the *R* configuration. Chiral pesticides can reduce application dosages compared to their corresponding racemic counterparts, thereby reducing environmental pollution.[10−12]

Carotenoids play an important role in many physiological processes of plants, and the phytoene desaturase gene (*PDS3*) is one of the important enzymes in the carotenoid synthesis pathway.[13] Eight commercially available bleaching herbicides target PDS (Figure 1), and they are widely used due to their efficacy, low resistance, and environmental friendliness. (*Rac*)-BF was developed by Cheminova in 2003 and applied in wheat

fields at a dosage of 170−255 g ai/ha to control broadleaf and common grass weeds.[3] (*Rac*)-BF is classified as a PDS herbicide and acts by inducing the accumulation of reactive oxygen species, which subsequently decompose chlorophyll and inhibit carotenoid biosynthesis under intense light irradiation. Severe carotenoid deficiency in leaves leads to leaf bleaching and eventual plant death.[14]

Based on the phenoxyamide structure of (*Rac*)-BF and the SAR studies, we further optimized the structure in order to discover candidate herbicide lead compounds with high activity, crop safety, and environmental friendliness. Additionally, we synthesized the chiral form of highly active compounds and compared its activity to that of the racemic compounds. The binding modes of the *S*configuration and *R*configuration compounds to PDS were analyzed through molecular docking studies. Furthermore, we investigated the degradation dynamics of (*S*)-BF in plants and analyzed its residual degradation half-life.
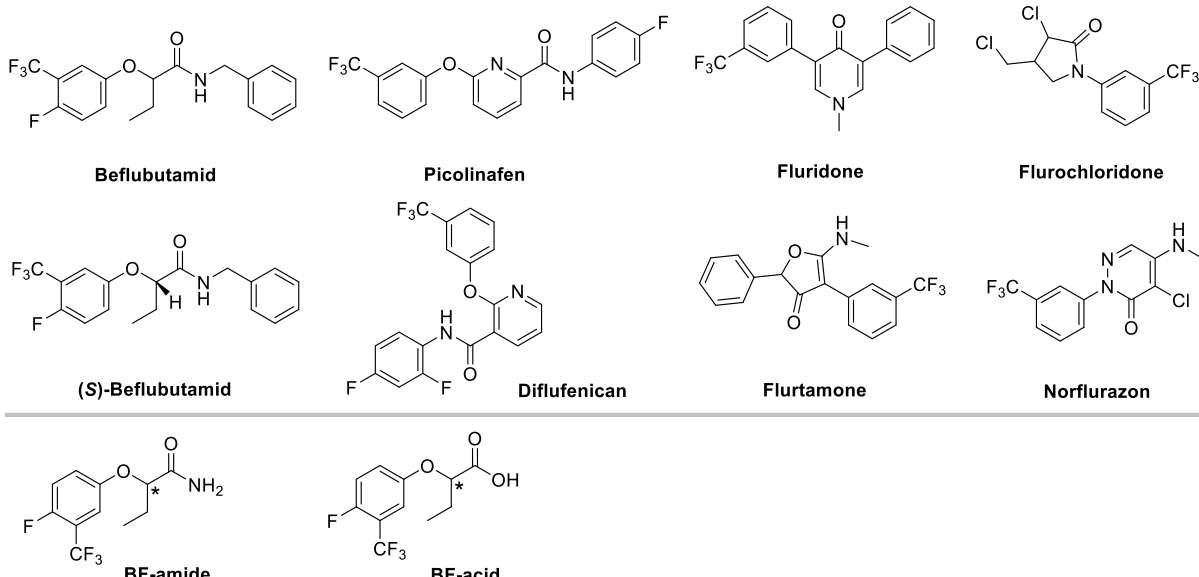
MATERIALS AND METHODS

Chemicals and Instruments. All of the chemical materials were purchased from Leyan (Beijing, China) or Bide (Shanghai, China) and used without further purification. ^{1}H, ^{19}F, and ^{13}C NMR spectra were acquired in chloroform-*d* or dimethyl sulfoxide-*d*₆ solutions using a Bruker Avance III 400 MHz spectrometer (Bruker BioSpin AG, Germany). High-resolution mass spectrometry analysis (HRMS)

Figure 1. Chemical structures of PDS-inhibiting herbicides (top and middle) and two metabolites of BF (BF-amide and BF-acid) that are formed in soils, plants, and animals (bottom). The asterisks indicate the asymmetrically substituted C atom of the chiral compounds.

was performed on a Thermo Fisher Q Exactive mass spectrometer (Thermo Fisher Scientific, USA). High-performance liquid chromatography (HPLC) analyses were conducted using a Shimadzu model SIL-20AC220 V instrument (Shimadzu, Japan). Liquid chromatograph–mass spectrometry (LC–MS) data were obtained using a 4000 Q TRAP instrument (AB Sciex, USA). Chiralcel brand chiral columns (Daicel Chemical Inc., Japan) with model ODH of 4.6 × 250 mm² size were employed. Optical rotations were measured in a 1 dm cuvette by using an Insmark IP-digi polarimeter (Shanghai, China). The melting points of all compounds were determined by using an X-4 binocular microscope (Beijing Tech Instruments Co., China). Single-crystal X-ray diffraction data were recorded on an Xcalibur Eos Gemini instrument (Agilent Technologies Inc., USA).

Synthesis of (R)-2-Bromobutanoic Acid.[15,16] At 0 °C, 48% HBr (20 mL) was added to a H₂O (18 mL) solution of (R)-2-aminobutyric acid (2.05 g, 20 mmol). The reaction mixture was stirred at 0 °C for 10 min, and NaNO₂ (2.1 g, 30 mmol) in a water (5 mL) solution was slowly added to the reaction solution. After stirring at 0 °C for 30 min, the reaction was allowed to proceed at room temperature for 3 h. After the reaction was complete, the reaction mixture was extracted with Et₂O (3 × 40 mL), the organic layer was washed with Na₂S₂O₃ (3 × 30 mL) and dried over anhydrous Na₂SO₄, the solid was filtered out, and the filtrate was concentrated under pressure to obtain (R)-2-bromobutanoic acid.

Synthesis of Ethyl (R)-2-Bromobutanoate.[17] To a mixture of (R)-2-bromobutanoic acid (1.5 g, 8.98 mmol), ethanol (4.2 mL, 71.86 mmol), and 2 mL of 1,2-dichloroethane (DCE), H₂SO₄ (0.5 mmol, 27 μL) was added at room temperature, and the reaction mixture was stirred at 90 °C for 1 h. The reactants were extracted with Et₂O (3 × 20 mL) and dried with anhydrous Na₂SO₄. The ethyl (R)-2-bromobutanoate was obtained after decompression and concentration.

General Procedures for the Synthesis of Compound 2.[18–20] To a round-bottomed flask, compound 1 (10 mmol), 30 mL of acetone, ethyl 2-bromobutyrate (9 mmol, 1.33 mL), and anhydrous potassium carbonate (25 mmol, 3.46 g) were added. The mixture was then refluxed for 10 h. Afterward, the reaction mixture was cooled to room temperature, and the solids were filtered out. The filtrate was dried and extracted with EtOAc (3 × 40 mL). The organic layer was washed with H₂O (3 × 30 mL) and saturated sodium chloride (3 × 30 mL). The organic phase was dried by using anhydrous sodium sulfate and concentrated under reduced pressure. The resulting residue was purified on silica gel using a petroleum ether/ethyl acetate (30:1) eluent to obtain the desired product.

*Ethyl 2-((4-Fluoro-3-(trifluoromethyl)phenyl)amino)butanoate (Rac)-**2**.* Colorless transparent liquid, yield 90%. ¹H NMR (400 MHz, chloroform-d) δ 7.13–7.05 (m, 2H), 7.05–6.98 (m, 1H), 4.54–4.49 (m, 1H), 4.22 (q, J = 7.1 Hz, 2H), 2.06–1.94 (m, 2H), 1.25 (t, J = 7.1 Hz, 3H), 1.08 (t, J = 7.4 Hz, 3H). HRMS (ESI): calcd for C₁₃H₁₄F₄O₃ [M + Na]⁺ 317.0771, found 317.0772.

General Procedures for the Synthesis of Compound 3.[18] Compound 2 was dissolved in a mixture of methanol (15 mL) and water (15 mL). To the solution was added lithium hydroxide (30 mmol, 0.72 g), and the mixture was stirred at room temperature for 4 h. After the reaction was completed, methanol was evaporated. The pH of the solution was adjusted to 2 to 3 using 6 M diluent hydrochloric acid, and the organic phase was extracted with EtOAc (3 × 30 mL). The organic phase was dried by using anhydrous sodium sulfate and concentrated under reduced pressure to obtain the product.

General Procedures for the Synthesis of Compound 4.[21,22] Compound 3 (1 mmol) was added to a round-bottomed flask along with 3 mL of ultradry methylene chloride solution. To this mixture, oxalyl chloride (1.5 mmol, 85 μL) was added, followed by the addition of 2 drops of N,N-dimethylformamide (DMF) after 30 min of reaction. The mixture was stirred at room temperature for 2 h, and then the reaction solution was concentrated to obtain the product.

General Procedures for the Synthesis of Compound 6.[23,24] At 0 °C, triethylamine (1.5 mmol, 0.15 g) was added to a solution of compound 5 (1 mmol) in dichloromethane (DCM, 4 mL). After stirring at 0 °C for 10 min, compound 4 (1 mmol) was added, and the mixture was stirred at room temperature for 3 h. After the reaction was completed, 30 mL of water was added to the mixture to separate the organic layer. The aqueous layer was extracted with DCM (3 × 20 mL). The organic layer was washed with saturated salt water (3 × 10 mL) and dried with anhydrous sodium sulfate, and the crude product was concentrated under vacuum. The mixture was then separated on silica gel and eluted with petroleum ether/ethyl acetate (5:1–1:1) to obtain the product.

*N-Benzyl-2-(4-fluoro-3-(trifluoromethyl)phenoxy)butanamide ((Rac)-**BF**).* White solid, yield 80%, mp 70–72 °C. ¹H NMR (400 MHz, DMSO-d₆) δ 8.73 (t, J = 6.1 Hz, 1H), 7.44 (m, 1H), 7.34–7.18 (m, 5H), 7.18–7.08 (m, 2H), 4.72 (t, J = 6.0 Hz, 1H), 4.37–4.23 (m, 2H), 1.95–1.82 (m, 2H), 0.97 (t, J = 7.4 Hz, 3H). ¹³C NMR (101 MHz, DMSO-d₆) δ 170.3, 154.2 (d, J = 2.2 Hz), 153.7 (d, J = 244.6 Hz), 139.7, 128.6, 127.4, 127.2, 122.8 (d, J = 271.9 Hz), 122.1 (q, J = 8.2 Hz), 118.7 (d, J = 22.1 Hz), 117.4 (dd, J = 32.6, 13.9 Hz), 114.0 (q, J = 5.0 Hz), 79.9, 42.3, 26.1, 9.7. ¹⁹F NMR (376 MHz, DMSO-d₆)

δ −60.3 (d, J = 11.3 Hz), −126.0 (q, J = 15.0 Hz). HRMS (ESI): calcd for $C_{18}H_{17}F_4NO_2$ [M + Na]$^+$ 378.1088, found 378.1091.

2-(4-Fluoro-3-(trifluoromethyl)phenoxy)-N-(pyrimidin-2-ylmethyl)butanamide ((Rac)-6a). Light-brown solid, yield 80%, mp 80−82 °C. ^{1}H NMR (400 MHz, DMSO-d_6) δ 8.80−8.68 (m, 3H), 7.47 (t, J = 9.7 Hz, 1H), 7.41−7.34 (m, 2H), 7.33−7.29 (m, 1H), 4.73−4.68 (m, 1H), 4.49 (d, J = 6.0 Hz, 2H), 1.95−1.82 (m, 2H), 1.00 (t, J = 7.4 Hz, 3H). ^{13}C NMR (101 MHz, DMSO-d_6) δ 170.7, 167.1, 157.7, 154.3 (d, J = 2.4 Hz), 153.7 (d, J = 243.1 Hz), 122.9 (d, J = 273.2 Hz), 122.1 (d, J = 8.4 Hz), 120.3, 118.6 (d, J = 22.0 Hz), 117.4 (dd, J = 32.6, 13.9 Hz), 114.4 (q, J = 4.8 Hz), 80.1, 44.9, 26.2, 9.7. HRMS (ESI): calcd for $C_{16}H_{15}F_4N_3O_2$ [M + Na]$^+$ 380.0993, found 380.0994.

N-([1,1′-Biphenyl]-4-ylmethyl)-2-(4-fluoro-3-(trifluoromethyl)phenoxy)butanamide ((Rac)-6b). White solid, yield 74%, mp 91−93 °C. ^{1}H NMR (400 MHz, DMSO-d_6) δ 8.76 (t, J = 6.1 Hz, 1H), 7.64−7.59 (m, 2H), 7.57−7.51 (m, 2H), 7.50−7.42 (m, 3H), 7.38−7.25 (m, 3H), 7.25−7.18 (m, 2H), 4.73 (t, J = 6.0 Hz, 1H), 4.39−4.27 (m, 2H), 1.93−1.84 (m, 2H), 0.97 (t, J = 7.4 Hz, 3H). ^{13}C NMR (101 MHz, DMSO-d_6) δ 170.4, 154.2 (d, J = 2.3 Hz), 153.8 (d, J = 244.3 Hz), 140.4, 139.2, 139.0, 129.4, 128.1, 127.8, 127.0, 126.9, 122.9 (q, J = 270.7 Hz), 122.1 (d, J = 8.2 Hz), 118.7 (d, J = 22.1 Hz), 117.4 (dd, J = 33.0, 13.7 Hz), 114.1 (q, J = 4.6 Hz), 80.0, 42.0, 26.1, 9.8. HRMS (ESI): calcd for $C_{24}H_{21}F_4NO_2$ [M + Na]$^+$ 454.1401, found 454.1400.

N-(4-Cyanobenzyl)-2-(4-fluoro-3-(trifluoromethyl)phenoxy)-butanamide ((Rac)-6c). White solid, yield 79%, mp 70−72 °C. ^{1}H NMR (400 MHz, DMSO-d_6) δ 8.83 (t, J = 6.2 Hz, 1H), 7.75−7.68 (m, 2H), 7.45 (t, J = 9.7 Hz, 1H), 7.36−7.20 (m, 4H), 4.76−4.70 (m, 1H), 4.41−4.29 (m, 2H), 1.92−1.82 (m, 2H), 0.95 (t, J = 7.4 Hz, 3H). ^{13}C NMR (101 MHz, DMSO-d_6) δ 170.6, 154.1 (d, J = 2.2 Hz), 153.8 (d, J = 244.4 Hz), 145.7, 132.6, 128.4, 122.8 (q, J = 271.7 Hz), 122.0 (d, J = 8.3 Hz), 119.3, 118.8 (d, J = 22.1 Hz), 117.4 (dd, J = 32.3, 13.5 Hz), 114.1 (q, J = 4.6 Hz), 110.0, 79.9, 42.1, 26.0, 9.7. HRMS (ESI): calcd for $C_{19}H_{16}F_4N_2O_2$ [M + Na]$^+$ 403.1040, found 403.1039.

2-(4-Fluoro-3-(trifluoromethyl)phenoxy)-N-(4-phenoxybenzyl)-butanamide ((Rac)-6d). Light-yellow solid, yield 76%, mp 81−83 °C. ^{1}H NMR (400 MHz, DMSO-d_6) δ 8.72 (t, J = 6.1 Hz, 1H), 7.47−7.34 (m, 3H), 7.32−7.23 (m, 2H), 7.18−7.09 (m, 3H), 6.98−6.93 (m, 2H), 6.92−6.86 (m, 2H), 4.70 (t, J = 6.0 Hz, 1H), 4.35−4.18 (m, 2H), 1.92−1.81 (m, 2H), 0.95 (t, J = 7.4 Hz, 3H). ^{13}C NMR (101 MHz, DMSO-d_6) δ 170.3, 157.3, 155.8, 154.1 (d, J = 2.4 Hz), 153.7 (d, J = 244.3 Hz), 134.9, 130.4, 129.2, 123.8, 122.8 (d, J = 271.8 Hz), 122.0 (d, J = 8.5 Hz), 119.0, 118.8, 118.7 (d, J = 22.1 Hz), 117.4 (dd, J = 32.5, 13.8 Hz), 114.0 (q, J = 4.6 Hz), 79.9, 41.7, 26.1, 9.7. HRMS (ESI): calcd for $C_{24}H_{21}F_4NO_3$ [M + Na]$^+$ 470.1350, found 470.1350.

N-(Benzo[d][1,3]dioxol-5-ylmethyl)-2-(4-fluoro-3-(trifluoromethyl)phenoxy)butanamide ((Rac)-6e). Light-yellow solid, yield 79%, mp 76−78 °C. ^{1}H NMR (400 MHz, DMSO-d_6) δ 8.65 (t, J = 6.1 Hz, 1H), 7.42 (t, J = 9.7 Hz, 1H), 7.32−7.18 (m, 2H), 6.77 (d, J = 7.9 Hz, 1H), 6.65 (d, J = 1.7 Hz, 1H), 6.61 (dd, J = 7.9, 1.7 Hz, 1H), 5.95 (q, J = 1.0 Hz, 2H), 4.68 (t, J = 6.0 Hz, 1H), 4.25−4.11 (m, 2H), 1.90−1.80 (m, 2H), 0.94 (t, J = 7.4 Hz, 3H). ^{13}C NMR (101 MHz, DMSO-d_6) δ 170.2, 154.1 (d, J = 2.2 Hz), 153.7 (d, J = 243.3 Hz), 147.6, 146.5, 133.6, 122.8 (q, J = 271.6 Hz), 122.0 (d, J = 8.6 Hz), 120.7, 118.7 (d, J = 22.1 Hz), 117.4 (dd, J = 32.5, 13.8 Hz), 114.0 (q, J = 4.8 Hz), 108.3, 108.1, 101.3, 79.9, 42.1, 26.0, 9.7. HRMS (ESI): calcd for $C_{19}H_{17}F_4NO_4$ [M + Na]$^+$ 422.0986, found 422.0986.

2-(4-Fluoro-3-(trifluoromethyl)phenoxy)-N-(pyrazin-2-ylmethyl)-butanamide ((Rac)-6f). Yellow solid, yield 75%, mp 67−69 °C. ^{1}H NMR (400 MHz, DMSO-d_6) δ 8.88 (t, J = 6.0 Hz, 1H), 8.57−8.48 (m, 2H), 8.43 (d, J = 1.5 Hz, 1H), 7.45 (t, J = 9.7 Hz, 1H), 7.36−7.24 (m, 2H), 4.75 (t, J = 5.9 Hz, 1H), 4.52−4.38 (m, 2H), 1.95−1.82 (m, 2H), 0.97 (t, J = 7.4 Hz, 3H). ^{13}C NMR (101 MHz, DMSO-d_6) δ 170.8, 154.3, 154.1 (d, J = 2.2 Hz), 153.7 (d, J = 246.1 Hz), 144.3, 143.6 (d, J = 1.8 Hz), 122.8 (q, J = 272.1 Hz), 122.0 (d, J = 8.4 Hz), 118.7 (d, J = 22.1 Hz), 117.4 (dd, J = 32.5, 13.9 Hz), 114.2 (q, J = 5.5 Hz), 79.9, 42.4, 26.0, 9.6. HRMS (ESI): calcd for $C_{16}H_{15}F_4N_3O_2$ [M + Na]$^+$ 380.0993, found 380.0990.

2-(4-Fluoro-3-(trifluoromethyl)phenoxy)-N-(naphthalen-2-ylmethyl)butanamide ((Rac)-6g). White solid, yield 73%, mp 105−107 °C. ^{1}H NMR (400 MHz, DMSO-d_6) δ 8.84 (t, J = 6.1 Hz, 1H), 7.91−7.84 (m, 1H), 7.81 (d, J = 8.4 Hz, 1H), 7.78−7.71 (m, 1H), 7.58 (s, 1H), 7.53−7.41 (m, 3H), 7.36−7.27 (m, 3H), 4.76 (t, J = 6.0 Hz, 1H), 4.56−4.38 (m, 2H), 1.97−1.83 (m, 2H), 0.98 (t, J = 7.4 Hz, 3H). ^{13}C NMR (101 MHz, DMSO-d_6) δ 170.5, 154.2 (d, J = 2.4 Hz), 153.7 (d, J = 245.3 Hz), 137.3, 133.2, 132.5, 128.3, 128.0, 127.8, 126.6, 126.1, 126.0, 125.6, 122.8 (q, J = 272.7 Hz), 121.9 (d, J = 8.1 Hz), 118.7 (d, J = 22.1 Hz), 117.5 (dd, J = 32.5, 13.9 Hz), 114.2 (q, J = 4.7 Hz), 80.0, 42.5, 26.1, 9.7. HRMS (ESI): calcd for $C_{22}H_{19}F_4NO_2$ [M + Na]$^+$ 428.1244, found 428.1239.

N-(Cyclohexylmethyl)-2-(4-fluoro-3-(trifluoromethyl)phenoxy)-butanamide ((Rac)-6h). White solid, yield 69%, mp 70−72 °C. ^{1}H NMR (400 MHz, DMSO-d_6) δ 8.12 (t, J = 6.0 Hz, 1H), 7.44 (t, J = 9.7 Hz, 1H), 7.32−7.18 (m, 2H), 4.61 (t, J = 6.2 Hz, 1H), 2.99−2.80 (m, 2H), 1.88−1.76 (m, 2H), 1.64−1.41 (m, 5H), 1.38−1.24 (m, 1H), 1.15−1.00 (m, 3H), 0.95 (t, J = 7.4 Hz, 3H), 0.82−0.68 (m, 2H). ^{13}C NMR (101 MHz, DMSO-d_6) δ 170.0, 154.2 (d, J = 2.2 Hz), 153.7 (d, J = 244.2 Hz), 122.9 (q, J = 272.3 Hz), 122.2 (d, J = 8.4 Hz), 118.7 (d, J = 22.2 Hz), 117.3 (dd, J = 32.5, 13.8 Hz), 113.7 (q, J = 4.9 Hz), 80.1, 44.9, 37.9, 30.7, 26.4, 26.2, 25.8 (d, J = 2.9 Hz), 9.8. HRMS (ESI): calcd for $C_{18}H_{23}F_4NO_2$ [M + Na]$^+$ 384.1557, found 384.1555.

N-(Benzyloxy)-2-(4-fluoro-3-(trifluoromethyl)phenoxy)-butanamide ((Rac)-6i). White solid, yield 76%, mp 75−77 °C. ^{1}H NMR (400 MHz, DMSO-d_6) δ 11.49 (s, 1H), 7.48−7.40 (m, 1H), 7.38−7.29 (m, 5H), 7.28−7.22 (m, 2H), 4.76 (s, 2H), 4.59 (t, J = 6.2 Hz, 1H), 1.88−1.77 (m, 2H), 0.92 (t, J = 7.4 Hz, 3H). ^{13}C NMR (101 MHz, DMSO-d_6) δ 166.9, 154.0 (d, J = 2.4 Hz), 153.8 (d, J = 246.9 Hz), 136.1, 129.3, 128.8, 128.7, 122.8 (q, J = 272.3 Hz), 121.9 (d, J = 8.4 Hz), 118.7 (d, J = 22.1 Hz), 117.5 (dd, J = 32.5, 14.1 Hz), 114.3 (q, J = 4.9 Hz), 78.5, 77.4, 26.0, 9.5. HRMS (ESI): calcd for $C_{18}H_{17}F_4NO_3$ [M + Na]$^+$ 394.1037, found 394.1038.

2-(4-Fluoro-3-(trifluoromethyl)phenoxy)-N-((4-methoxybenzyl)-oxy)butanamide ((Rac)-6j). White solid, yield 66%, mp 64−66 °C. ^{1}H NMR (400 MHz, DMSO-d_6) δ 11.42 (s, 1H), 7.45 (t, J = 9.8 Hz, 1H), 7.29−7.20 (m, 4H), 6.92−6.86 (m, 2H), 4.68 (s, 2H), 4.58 (t, J = 6.2 Hz, 1H), 3.75 (s, 3H), 1.91−1.71 (m, 2H), 0.93 (t, J = 7.4 Hz, 3H). ^{13}C NMR (101 MHz, DMSO-d_6) δ 166.9, 159.9, 154.0 (d, J = 2.4 Hz), 153.8 (d, J = 246.0 Hz), 131.1, 128.0, 122.8 (q, J = 272.5 Hz), 121.8 (d, J = 8.4 Hz), 118.7 (d, J = 22.2 Hz), 117.5 (dd, J = 32.5, 13.9 Hz), 114.3 (q, J = 5.3 Hz), 114.1, 78.5, 77.0, 55.5, 26.0, 9.6. HRMS (ESI): calcd for $C_{19}H_{19}F_4NO_4$ [M + Na]$^+$ 424.1142, found 424.1141.

2-(4-Fluoro-3-(trifluoromethyl)phenoxy)-N-((4-fluorobenzyl)-oxy)butanamide ((Rac)-6k). White solid, yield 76%, mp 88−90 °C. ^{1}H NMR (400 MHz, DMSO-d_6) δ 11.47 (s, 1H), 7.49−7.41 (m, 1H), 7.41−7.34 (m, 2H), 7.29−7.20 (m, 2H), 7.20−7.10 (m, 2H), 4.75 (s, 2H), 4.59 (t, J = 6.2 Hz, 1H), 1.88−1.76 (m, 2H), 0.92 (t, J = 7.4 Hz, 3H). ^{13}C NMR (101 MHz, DMSO-d_6) δ 167.0, 162.6 (d, J = 244.4 Hz), 153.9, 153.8 (d, J = 245.7 Hz), 132.4 (d, J = 3.3 Hz), 131.5 (d, J = 8.4 Hz), 122.8 (q, J = 272.2 Hz), 121.8 (d, J = 8.4 Hz), 118.7 (d, J = 22.1 Hz), 117.5 (qd, J = 32.4, 13.7 Hz), 115.6, 115.4, 114.3 (q, J = 5.1 Hz), 78.5, 76.5, 26.0, 9.5. ^{19}F NMR (376 MHz, DMSO-d_6) δ −60.3 (d, J = 12.6 Hz), −113.8, −125.8 (q, J = 12.8 Hz). HRMS (ESI): calcd for $C_{18}H_{16}F_5NO_3$ [M + Na]$^+$ 412.0943, found 412.0943.

2-(4-Fluoro-3-(trifluoromethyl)phenoxy)-N-((4-(trifluoromethyl)-benzyl)oxy)butanamide ((Rac)-6l). White solid, yield 72%, mp 85−87 °C. ^{1}H NMR (400 MHz, DMSO-d_6) δ 11.59 (s, 1H), 7.73 (d, J = 7.6 Hz, 2H), 7.60 (d, J = 8.6 Hz, 2H), 7.50−7.41 (m, 1H), 7.30−7.22 (m, 2H), 4.92 (s, 2H), 4.64 (t, J = 6.2 Hz, 1H), 1.92−1.81 (m, 2H), 0.95 (t, J = 7.4 Hz, 3H). ^{13}C NMR (101 MHz, DMSO-d_6) δ 166.5, 153.3 (d, J = 2.3 Hz), 153.1 (d, J = 245.6 Hz), 140.3, 129.0, 128.5 (d, J = 31.7 Hz), 124.9 (q, J = 3.8 Hz), 124.0 (q, J = 272.1 Hz), 122.1 (q, J = 272.3 Hz), 121.1 (d, J = 8.5 Hz), 118.1 (d, J = 22.2 Hz), 116.8 (dd, J = 32.6, 13.9 Hz), 113.6 (q, J = 4.8 Hz), 77.9, 75.7, 25.3, 8.8. ^{19}F NMR (376 MHz, DMSO-d_6) δ −60.3 (d, J = 13.0 Hz), −61.2, −125.8 (q, J = 12.8 Hz). HRMS (ESI): calcd for $C_{19}H_{16}F_7NO_3$ [M + Na]$^+$ 462.0911, found 462.0915.

C

N-((2,4-Dichlorobenzyl)oxy)-2-(4-fluoro-3-(trifluoromethyl)-phenoxy)butanamide ((Rac)-6m). White solid, yield 70%, mp 94−96 °C. ^{1}H NMR (400 MHz, DMSO-d_6) δ 11.59 (s, 1H), 7.67 (d, J = 2.1 Hz, 1H), 7.54−7.41 (m, 3H), 7.33−7.25 (m, 2H), 4.92 (s, 2H), 4.64 (t, J = 6.2 Hz, 1H), 1.98−1.79 (m, 2H), 0.97 (t, J = 7.4 Hz, 3H). ^{13}C NMR (101 MHz, DMSO-d_6) δ 167.2, 153.9 (d, J = 2.2 Hz), 153.8 (d, J = 247.1 Hz), 134.6, 134.3, 132.9 (d, J = 4.3 Hz), 129.2, 127.7, 122.8 (q, J = 272.5 Hz), 121.8 (d, J = 8.3 Hz), 118.7 (d, J = 22.1 Hz), 117.4 (dd, J = 32.6, 13.7 Hz), 114.3 (q, J = 4.9 Hz), 78.5, 73.6, 26.0, 9.6.HRMS (ESI): calcd for $C_{18}H_{15}Cl_2F_4NO_3$ [M + Na]$^+$ 462.0257, found 462.0253.

2-(4-Fluoro-3-(trifluoromethyl)phenoxy)-N-phenylbutanamide ((Rac)-6n). White solid, yield 79%, mp 109−111 °C. ^{1}H NMR (400 MHz, DMSO-d_6) δ 10.15 (s, 1H), 7.63−7.55 (m, 2H), 7.53−7.40 (m, 1H), 7.37−7.26 (m, 4H), 7.13−7.04 (m, 1H), 4.81 (t, J = 6.2 Hz, 1H), 2.01−1.90 (m, 2H), 1.02 (t, J = 7.4 Hz, 3H). ^{13}C NMR (101 MHz, DMSO-d_6) δ 169.1, 154.2 (d, J = 2.3 Hz), 153.7 (d, J = 246.4 Hz), 138.6, 129.2, 124.4, 122.8 (q, J = 272.1 Hz), 121.7 (d, J = 8.3 Hz), 120.4, 118.9 (d, J = 22.2 Hz), 117.5 (dd, J = 32.6, 13.9 Hz), 114.2 (q, J = 4.7 Hz), 80.0, 26.1, 9.8. HRMS (ESI): calcd for $C_{17}H_{15}F_4NO_2$ [M + Na]$^+$ 364.0931, found 364.0927.

N-(2-Ethyl-6-methylphenyl)-2-(4-fluoro-3-(trifluoromethyl)-phenoxy)butanamide ((Rac)-6o). White solid, yield 74%, mp 123−125 °C. ^{1}H NMR (400 MHz, DMSO-d_6) δ 9.52 (s, 1H), 7.57−7.32 (m, 3H), 7.18−6.97 (m, 3H), 4.91−4.83 (m, 1H), 2.38−2.17 (m, 2H), 2.09−1.90 (m, 5H), 1.10 (t, J = 7.4 Hz, 3H), 0.91 (t, J = 7.6 Hz, 3H). ^{13}C NMR (101 MHz, DMSO-d_6) δ 169.6, 154.3 (d, J = 2.4 Hz), 153.9 (d, J = 247.9 Hz), 141.7, 136.1, 134.1, 128.2, 127.6, 126.6, 122.9 (q, J = 272.4 Hz), 122.4 (d, J = 8.3 Hz), 118.8 (d, J = 22.2 Hz), 117.3 (dd, J = 32.4, 13.9 Hz), 113.8 (q, J = 5.0 Hz), 80.3, 26.6, 24.6, 18.4, 14.9, 10.1. HRMS (ESI): calcd for $C_{20}H_{21}F_4NO_2$ [M + Na]$^+$ 406.1401, found 406.1393.

N-(4,6-Dimethoxypyrimidin-2-yl)-2-(4-fluoro-3-(trifluoromethyl)-phenoxy)butanamide ((Rac)-6p). White solid, yield 70%, mp 78−80 °C. ^{1}H NMR (400 MHz, DMSO-d_6) δ 10.73 (s, 1H), 7.52−7.42 (m, 1H), 7.28−7.21 (m, 2H), 5.97 (s, 1H), 5.20 (t, J = 6.1 Hz, 1H), 3.87 (s, 6H), 2.07−1.80 (m, 2H), 1.03 (t, J = 7.4 Hz, 3H). ^{13}C NMR (101 MHz, DMSO-d_6) δ 172.1, 169.2, 156.6, 154.2 (d, J = 2.3 Hz), 153.6 (d, J = 245.8 Hz), 122.8 (q, J = 272.3 Hz), 121.2 (d, J = 8.4 Hz), 118.9 (d, J = 22.2 Hz), 117.6 (dd, J = 32.6, 13.9 Hz), 113.8 (q, J = 4.7 Hz), 85.0, 78.9, 54.6, 26.0, 10.0. HRMS (ESI): calcd for $C_{17}H_{17}F_4N_3O_4$ [M + Na]$^+$ 426.1047, found 426.1039.

2-(4-Fluoro-3-(trifluoromethyl)phenoxy)-N-(1H-1,2,4-triazol-3-yl)butanamide ((Rac)-6q). White solid, yield 80%, mp 109−111 °C. ^{1}H NMR (400 MHz, DMSO-d_6) δ 7.70 (d, J = 17.9 Hz, 3H), 7.43 (t, J = 9.6 Hz, 1H), 7.33−7.17 (m, 2H), 5.72 (dd, J = 7.4, 4.1 Hz, 1H), 2.19−2.07 (m, 1H), 2.05−1.92 (m, 1H), 1.04 (t, J = 7.4 Hz, 3H). ^{13}C NMR (101 MHz, DMSO-d_6) δ 170.6, 157.8, 153.9 (d, J = 2.2 Hz), 153.9 (d, J = 244.7 Hz), 152.8, 125.4 (q, J = 272.3 Hz), 121.3 (d, J = 8.2 Hz), 119.0 (d, J = 22.2 Hz), 117.7 (dd, J = 32.5, 14.0 Hz), 114.3 (q, J = 4.8 Hz), 77.6, 25.5, 9.8. HRMS (ESI): calcd for $C_{13}H_{12}F_4N_4O_2$ [M + Na]$^+$ 355.0789, found 355.0782.

N-Benzyl-2-((1-methyl-3-(trifluoromethyl)-1H-pyrazol-5-yl)oxy)-butanamide ((Rac)-6r). White solid, yield 69%, mp 72−74 °C. ^{1}H NMR (400 MHz, DMSO-d_6) δ 8.75 (t, J = 6.1 Hz, 1H), 7.31−7.20 (m, 3H), 7.20−7.14 (m, 2H), 6.06 (s, 1H), 4.67 (t, J = 6.0 Hz, 1H), 4.41−4.24 (m, 2H), 3.70 (s, 3H), 1.98−1.82 (m, 2H), 0.96 (t, J = 7.4 Hz, 3H). ^{13}C NMR (101 MHz, DMSO-d_6) δ 169.2, 153.9, 139.6, 138.6 (q, J = 37.6 Hz), 128.7, 127.5, 127.3, 121.7 (q, J = 268.0 Hz), 85.5 (q, J = 2.3 Hz), 83.0, 42.4, 34.9, 25.7, 9.5. ^{19}F NMR (376 MHz, DMSO-d_6) δ −61.4. HRMS (ESI): calcd for $C_{16}H_{18}F_3N_3O_2$ [M + Na]$^+$ 364.1243, found 364.1240.

N-Benzyl-2-((2-(trifluoromethyl)pyridin-4-yl)oxy)butanamide ((Rac)-6s). White solid, yield 75%, mp 65−67 °C. ^{1}H NMR (400 MHz, DMSO-d_6) δ 8.80 (t, J = 6.0 Hz, 1H), 8.57 (d, J = 5.7 Hz, 1H), 7.40 (d, J = 2.5 Hz, 1H), 7.31−7.19 (m, 4H), 7.19−7.11 (m, 2H), 4.94 (t, J = 6.0 Hz, 1H), 4.30 (d, J = 6.0 Hz, 2H), 2.00−1.83 (m, 2H), 0.96 (t, J = 7.4 Hz, 3H). ^{13}C NMR (101 MHz, DMSO-d_6) δ 169.5, 165.3, 152.2, 148.5 (q, J = 33.7 Hz), 139.6, 128.7, 127.5, 127.3, 121.9 (q, J = 274.3 Hz), 114.1, 108.9 (q, J = 2.9 Hz), 79.1, 42.4, 25.9, 9.6.

^{19}F NMR (376 MHz, DMSO-d_6) δ −66.8. HRMS (ESI): calcd for $C_{17}H_{17}F_3N_2O_2$ [M + Na]$^+$ 361.1134, found 361.1134.

N-Benzyl-2-((6-chloro-3-phenylpyridazin-4-yl)oxy)butanamide ((Rac)-6t). White solid, yield 68%, mp 154−156 °C. ^{1}H NMR (400 MHz, DMSO-d_6) δ 8.82 (t, J = 6.0 Hz, 1H), 7.98−7.91 (m, 2H), 7.56−7.48 (m, 3H), 7.36−7.29 (m, 3H), 7.29−7.19 (m, 3H), 5.07 (t, J = 5.8 Hz, 1H), 4.42−4.25 (m, 2H), 1.97−1.86 (m, 2H), 0.90 (t, J = 7.4 Hz, 3H). ^{13}C NMR (101 MHz, DMSO-d_6) δ 168.6, 156.3, 155.0, 152.9, 139.5, 133.9, 130.1, 129.8, 128.8, 128.6, 127.5, 127.4, 111.1, 79.5, 42.6, 25.7, 9.5. HRMS (ESI): calcd for $C_{17}H_{17}F_3N_2O_2$ [M + Na]$^+$ 404.1136, found 404.1134.

N-Benzyl-2-(4-(3-chloro-5-(trifluoromethyl)pyridin-2-yl)-phenoxy)butanamide ((Rac)-6u). White solid, yield 72%, mp 127−129 °C. ^{1}H NMR (400 MHz, DMSO-d_6) δ 9.05−8.97 (m, 1H), 8.72 (t, J = 6.1 Hz, 1H), 8.54 (dd, J = 2.1, 0.8 Hz, 1H), 7.78−7.67 (m, 2H), 7.34−7.12 (m, 5H), 7.13−7.02 (m, 2H), 4.70 (t, J = 6.1 Hz, 1H), 4.40−4.22 (m, 2H), 1.96−1.82 (m, 2H), 0.99 (t, J = 7.4 Hz, 3H). ^{13}C NMR (101 MHz, DMSO-d_6) δ 170.7, 159.3, 159.2, 144.9 (q, J = 4.3 Hz), 139.8, 136.3 (q, J = 3.6 Hz), 131.4, 130.0, 129.7, 128.7, 127.5, 127.2, 124.9 (q, J = 33.5 Hz), 122.0, 115.3, 79.2, 42.3, 26.3, 9.9. ^{19}F NMR (376 MHz, DMSO-d_6) δ −60.5. HRMS (ESI): calcd for $C_{23}H_{20}ClF_3N_2O_2$ [M + Na]$^+$ 471.1058, found 471.1058.

N-Benzyl-2-((4'-fluoro-3'-(trifluoromethyl)-[1,1'-biphenyl]-4-yl)-oxy)butanamide ((Rac)-6v). Yellow solid, yield 75%, mp 115−117 °C. ^{1}H NMR (400 MHz, DMSO-d_6) δ 8.69 (t, J = 6.1 Hz, 1H), 8.03−7.95 (m, 1H), 7.92 (dd, J = 7.0, 2.4 Hz, 1H), 7.71−7.63 (m, 2H), 7.62−7.54 (m, 1H), 7.30−7.23 (m, 2H), 7.23−7.14 (m, 3H), 7.09−7.03 (m, 2H), 4.66 (t, J = 6.1 Hz, 1H), 4.37−4.25 (m, 2H), 1.95−1.84 (m, 2H), 0.98 (t, J = 7.4 Hz, 3H). ^{13}C NMR (101 MHz, Chloroform-d) δ 175.6, 163.0, 144.6, 142.1 (d, J = 3.7 Hz), 138.0 (d, J = 8.4 Hz), 135.9, 133.4 (d, J = 2.1 Hz), 132.3, 131.9, 129.8 (q, J = 5.1 Hz), 127.9 (q, J = 272.3 Hz), 122.9 (d, J = 20.4 Hz), 122.2 (dd, J = 32.1, 12.4 Hz), 121.1, 84.1, 47.0, 31.0, 14.6. ^{19}F NMR (376 MHz, DMSO-d_6) δ −60.0 (d, J = 12.5 Hz), −119.3 − −119.5 (m). HRMS (ESI): calcd for $C_{24}H_{21}F_4NO_2$ [M + Na]$^+$ 454.1401, found 454.1388.

(S)-N-Benzyl-2-(4-fluoro-3-(trifluoromethyl)phenoxy)-butanamide ((S)-BF). White solid, yield 67%, mp 70−72 °C. $[\alpha]^{25}_D$ = −29.93 (c = 0.5 in CHCl$_3$). ^{1}H NMR (400 MHz, chloroform-d) δ 7.33−7.23 (m, 3H), 7.20−7.07 (m, 4H), 7.06−6.99 (m, 1H), 6.59 (s, 1H), 4.54 (dd, J = 6.5, 4.7 Hz, 1H), 4.47 (d, J = 5.9 Hz, 2H), 2.07−1.93 (m, 2H), 1.04 (t, J = 7.4 Hz, 3H). ^{13}C NMR (101 MHz, chloroform-d) δ 170.6, 154.6 (d, J = 250.7 Hz), 153.1 (d, J = 2.6 Hz), 137.7, 128.8, 127.7, 127.6, 122.1 (q, J = 272.8 Hz), 120.0 (d, J = 8.4 Hz), 119.2 (dd, J = 33.3, 14.2 Hz), 118.1 (d, J = 22.4 Hz), 114.4 (q, J = 3.0 Hz), 81.1, 43.1, 26.1, 9.3. HRMS (ESI): calcd for $C_{18}H_{17}F_4NO_2$ [M + Na]$^+$ 378.1088, found 378.1088.

(S)-2-(4-Fluoro-3-(trifluoromethyl)phenoxy)-N-(pyrimidin-2-ylmethyl)butanamide ((S)-6a). White solid, yield 63%, mp 80−82 °C. $[\alpha]^{25}_D$ = −34.93 (c = 0.5 in CHCl$_3$). ^{1}H NMR (400 MHz, chloroform-d) δ 8.66 (d, J = 4.9 Hz, 2H), 7.55 (s, 1H), 7.30−7.24 (m, 1H), 7.22−7.17 (m, 1H), 7.16−7.07 (m, 2H), 4.81−4.63 (m, 2H), 4.55 (dd, J = 6.8, 4.6 Hz, 1H), 2.11−1.95 (m, 2H), 1.08 (t, J = 7.4 Hz, 3H). ^{13}C NMR (101 MHz, Chloroform-d) δ 170.9, 165.5, 157.2, 154.6 (d, J = 248.3 Hz), 153.6 (d, J = 2.6 Hz), 122.2 (q, J = 271.3 Hz), 120.4 (d, J = 8.1 Hz), 119.6, 119.1 (dd, J = 33.3, 14.1 Hz), 117.9 (d, J = 22.3 Hz), 115.0 (q, J = 3.0 Hz), 81.6, 44.7, 26.3, 9.4. HRMS (ESI): calcd for $C_{16}H_{15}F_4N_3O_2$ [M + Na]$^+$ 380.0993, found 380.0992.

(S)-N-(Cyclohexylmethyl)-2-(4-fluoro-3-(trifluoromethyl)-phenoxy)butanamide ((S)-6h). White solid, yield 61%, mp 70−72 °C. $[\alpha]^{25}_D$ = −5.67 (c = 0.5 in CHCl$_3$). ^{1}H NMR (400 MHz, DMSO-d_6) δ 8.13 (t, J = 6.0 Hz, 1H), 7.49−7.40 (m, 1H), 7.31−7.20 (m, 2H), 4.62 (t, J = 6.2 Hz, 1H), 3.01−2.90 (m, 1H), 2.90−2.80 (m, 1H), 1.89−1.77 (m, 2H), 1.65−1.41 (m, 5H), 1.36−1.27 (m, 1H), 1.14−1.00 (m, 3H), 0.96 (t, J = 7.4 Hz, 3H), 0.83−0.68 (m, 2H). ^{13}C NMR (101 MHz, DMSO-d_6) δ 170.0, 154.2 (d, J = 2.2 Hz), 153.7 (d, J = 244.1 Hz), 122.9 (q, J = 272.0 Hz), 122.2 (d, J = 8.2 Hz), 118.7 (d, J = 22.3 Hz), 117.3 (dd, J = 32.4, 13.8 Hz), 113.7 (q, J = 5.0 Hz), 80.1, 44.9, 37.9, 30.7, 26.4, 26.2, 25.8 (d, J = 2.9 Hz), 9.8. HRMS (ESI): calcd for $C_{18}H_{23}F_4NO_2$ [M + Na]$^+$ 384.1557, found 384.1561.

(S)-2-(4-Fluoro-3-(trifluoromethyl)phenoxy)-N-phenylbutanamide ((S)-6n). White solid, yield 69%, mp 109−111 °C. $[\alpha]^{25}_D$ = −2.60 (c = 0.5 in CHCl$_3$). ^{1}H NMR (400 MHz, chloroform-d) δ 8.01 (s, 1H), 7.57−7.49 (m, 2H), 7.38−7.30 (m, 2H), 7.24 (dd, J = 5.6, 2.9 Hz, 1H), 7.20−7.08 (m, 3H), 4.62−4.57 (m, 1H), 2.12−2.01 (m, 2H), 1.09 (t, J = 7.4 Hz, 3H). ^{13}C NMR (101 MHz, Chloroform-d) δ 168.8, 154.8 (d, J = 251.4 Hz), 153.0 (d, J = 2.7 Hz), 136.7, 129.1, 125.0, 122.1 (q, J = 272.8 Hz), 120.1, 120.1, 119.5 (dd, J = 33.4, 14.2 Hz), 118.3 (d, J = 22.5 Hz), 114.9 (q, J = 3.0 Hz), 81.5, 26.0, 9.2. HRMS (ESI): calcd for C$_{17}$H$_{15}$F$_4$NO$_2$ [M + Na]$^+$ 364.0931, found 364.0931.

(S)-2-(4-Fluoro-3-(trifluoromethyl)phenoxy)-N-(1H-1,2,4-triazol-3-yl)butanamide ((S)-6q). White solid, yield 66%, mp 109−111 °C. $[\alpha]^{25}_D$ = −10.40 (c = 0.25 in CHCl$_3$). ^{1}H NMR (400 MHz, chloroform-d) δ 7.53 (s, 1H), 7.18 (dd, J = 5.6, 3.1 Hz, 1H), 7.09 (t, J = 9.3 Hz, 1H), 7.04−6.97 (m, 1H), 6.83 (s, 2H), 5.60 (dd, J = 7.6, 4.1 Hz, 1H), 2.23−2.00 (m, 2H), 1.14 (t, J = 7.4 Hz, 3H). ^{13}C NMR (101 MHz, Chloroform-d) δ 171.6, 157.3, 154.5 (d, J = 252.6 Hz), 151.5, 122.2 (q, J = 271.7 Hz), 119.7 (d, J = 8.1 Hz), 119.2 (dd, J = 33.3, 14.1 Hz), 117.9 (d, J = 22.5 Hz), 114.5 (q, J = 4.0 Hz), 77.6, 25.8, 9.7. HRMS (ESI): calcd for C$_{13}$H$_{12}$F$_4$N$_4$O$_2$ [M + Na]$^+$ 355.0789, found 355.0781.

X-ray Diffraction. To confirm the structure of the synthesized chiral compound, a single crystal of compound (S)-6h was used for X-ray structure analysis. White single crystals were obtained from a mixture of petroleum ether and ethyl acetate for compound (S)-6h. The X-ray crystal structure of compound (S)-6h was shown in Figure 2. A transparent crystal of compound (S)-6h measuring 0.35 × 0.18 ×
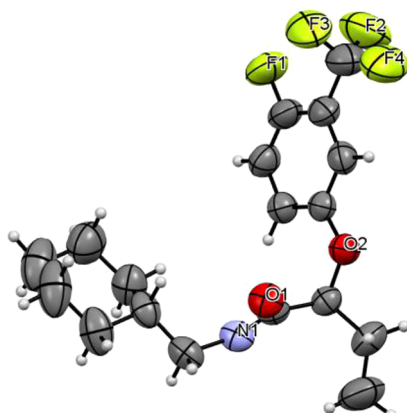
**Figure 2.** X-ray crystal structure of compound (S)-6h.

0.15 mm^3 was selected. It crystallized in the monoclinic space group P2$_1$2$_1$2$_1$, cell: a 12.0794 Å, b 17.7371 Å, c 17.7868 Å, α 103.543 (7)°, β 92.858 (9)°, γ 111.599 (11)°, and temperature 293 K. The crystallographic data of crystal (S)-6h have been deposited with the Cambridge Crystallographic Data Centre (CCDC) under deposition number 2262743. These data can be accessed free of charge at https://www.ccdc.cam.ac.uk.

HPLC Analysis Conditions. Chiralcel OD-H chiral columns (4.6 mm × 250 mm), column temperature 25 °C, sample room temperature 4 °C, injection volume 10 μL. Mobile phase A: hexane; mobile phase B: isopropyl alcohol (IPA). Compound (S)-BF (hexane/IPA = 95/5, flow rate 0.5 mL/min, 254 nm); t$_S$ major: 21.5 min; t$_R$ minor: 23.0 min; 82% ee. Compound (S)-6a (hexane/IPA = 90/10, flow rate 1 mL/min, 254 nm), t$_S$ major: 13.3 min; t$_R$ minor: 18.9 min; 76% ee. Compound (S)-6h (hexane/IPA = 97:3, flow rate 0.5 mL/min, 254 nm), t$_S$ major: 14.2 min; t$_R$ minor: 16.4 min; 74% ee. Compound (S)-6n (hexane/IPA = 97/3, flow rate 0.5 mL/min, 265 nm), t$_S$ major: 30.5 min; t$_R$ minor: 33.1 min; 74% ee. Compound (S)-6q (hexane/IPA = 97/3, flow rate 0.5 mL/min, 254 nm); t$_S$ major: 15.1 min; t$_R$ minor: 16.4 min; 70% ee.

Herbicidal Activity Assay.[25−27] In the initial round of experiments, herbicidal activities of compound (Rac)-6 were

evaluated against five weed species, namely, *Amaranthus retroflexus* (AR), *Abutilon theophrasti* (AT), *Medicago sativa* (MS), *Echinochloa crus-galli* (EC), and *Digitaria sanguinalis* (DS). In the subsequent round of experiments, the herbicidal activity of highly active compounds in both their (S)-configurations and their corresponding racemic forms was tested and compared. The evaluation concentrations for herbicidal activity were set to 150 and 300 g ai/ha. The experiment involves placing nutrient soil in a flower pot with an inner diameter of 7.0 cm and then sowing a specific number of weed seeds (germination rate ≥85%), covering them with 0.5 cm of nutrient soil, and cultivating them in a greenhouse at a temperature of 28 ± 1 °C and 80% relative humidity for 2 weeks.

The target compounds under investigation were dissolved and prepared as a 10000 mg/L mother solution using DMF, which were then diluted with water (containing 0.1% Tween-80) to the desired concentration. All treatments were repeated in three pots; (Rac)-BF, (S)-BF, and diflufenican (DF) were chosen as positive controls. After 21 days, the herbicidal efficacy of the tested inhibitors against the five weed species was assessed using a visual observation method.
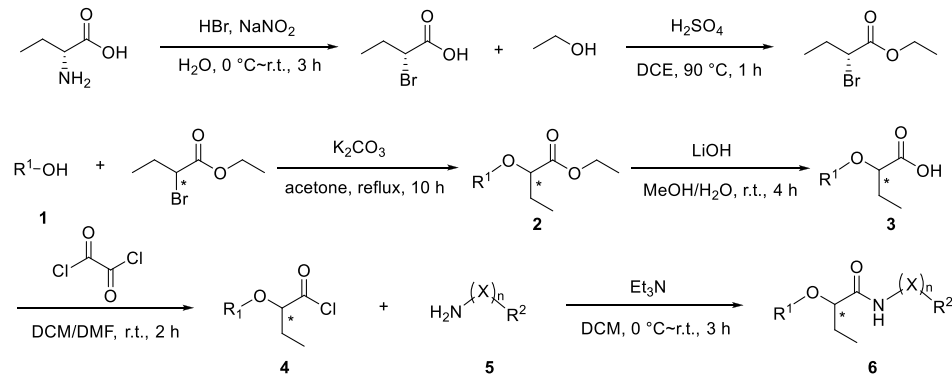
Determination of PDS Inhibitory Activity In Vivo. The Plant PDS ELISA Kit (MM-6265801, Jiangsu Meimian Industrial Co., Ltd., China) was used to detect the activity concentration of PDS in the leaves of AT. Specifically, when AT reached the fourth leaf stage, compound 6 was applied at a dosage of 300 g ai/ha, and leaf tissue was harvested 3 days postapplication. To prepare the leaf tissue for analysis, fresh leaves (fourth leaf, 0.1 g) of AT were ground into a fine powder using liquid nitrogen. Subsequently, 0.01 M phosphate-buffered saline (PBS) with a pH range of 7.2 to 7.4 was added to create a tissue homogenate: ratio of leaf tissue weight (g):PBS buffer volume (mL) = 1:9 to obtain 10% tissue homogenate. After that, the homogenate was centrifuged at 4000 rpm for 15 min to obtain the supernatant. The assessment of PDS inhibitory activity was conducted following the manufacturer's instructions provided with the PDS detection kit. Sequentially, the reaction reagents were added, and the optical density (OD) was measured at 450 nm using a plate reader (Multiskan FC). The activity concentration of PDS was subsequently calculated. In the blank control experiment, neither sample nor enzyme-labeled reagents were introduced, with all other steps identical to those employed in the assay.

Crop Selectivity Test.[25−27] Six conventional crops, wheat, rice, peanut, maize, soybeans, and cotton, were selected for crop selection experiments after greenhouse emergence. After filling three-quarters of a 10.0 cm pot with nutrient soil, put 10 seeds (germination rate ≥85%) in the pot. Cover the seeds with 1.0 cm of nutrient soil. Greenhouse environment conditions are the same as weed growth conditions. After 14 days of crop growth, a concentration of 300 g ai/ha was applied to test the crop safety of the compound, and each treatment was repeated three times. (Rac)-BF and (S)-BF were chosen as positive controls. The crop safety results were evaluated 14 days after administration.

Molecular Docking. The structures of compounds (R)-BF, (S)-BF, (R)-6h, and (S)-6h were constructed and optimized by Chem3D 20.0 before use. The crystal structure of OsPDS (PDB code: 5MOG) was downloaded from the Protein Data Bank (PDB) database. AutoDockTools version 1.5.6 was used to prepare the ligands and receptors and predict the binding modes. The Discovery Studio 2016 client is used to visualize simulation results on the interactions between compounds and receptors.[28]

Digestion Dynamics of (S)-BF in Wheat Plants.[29−31] The application of the pesticide was initiated at the three-leaf stage of wheat, with an application concentration of 150 g ai/ha. (S)-BF was dissolved with DMF and configured into 10000 mg/L mother liquor, which was diluted to the required concentration with 0.1% Tween-80 water. After the pesticide application, the blade surfaces were allowed to dry, sampling times were 0, 3, 6, 9, 12, 24, 72, 120, 168, and 300 h, and each treatment was replicated three times. Following sampling, the wheat blades were rapidly frozen using liquid nitrogen and stored at −80 °C for future use.

Chromatographic Conditions. The determination was carried out using an Agilent ZORBAX SB-C18 column, 5 μm, 4.6 × 150 mm^2,

Scheme 1. Synthesis of Compounds (*Rac*)-6, (*S*)-6a, (*S*)-6h, (*S*)-6n, and (*S*)-6q

Compds	N	X	R¹	R²	PDS inhibitory activity[a]
(*Rac*)-6a	1	CH₂	4-F-3-CF₃-Ph	pyrimidin-2-yl	180 ± 25
(*Rac*)-6b	1	CH₂	4-F-3-CF₃-Ph	[1,1'-biphenyl]-4-yl	605 ± 25
(*Rac*)-6c	1	CH₂	4-F-3-CF₃-Ph	4-cyanophenyl	393 ± 38
(*Rac*)-6d	1	CH₂	4-F-3-CF₃-Ph	4-phenoxyphenyl	405 ± 20
(*Rac*)-6e	1	CH₂	4-F-3-CF₃-Ph	benzo[d][1,3]dioxol-5-yl	505 ± 20
(*Rac*)-6f	1	CH₂	4-F-3-CF₃-Ph	pyrazin-2-yl	495 ± 9
(*Rac*)-6g	1	CH₂	4-F-3-CF₃-Ph	naphthalen-2-yl	468 ± 13
(*Rac*)-6h	1	CH₂	4-F-3-CF₃-Ph	CH(CH₂)₅	118 ± 15
(*Rac*)-6i	1	O	4-F-3-CF₃-Ph	CH₂Ph	630 ± 25
(*Rac*)-6j	1	O	4-F-3-CF₃-Ph	4-OCH₃-CH₂Ph	582 ± 25
(*Rac*)-6k	1	O	4-F-3-CF₃-Ph	4-F-CH₂Ph	418 ± 33
(*Rac*)-6l	1	O	4-F-3-CF₃-Ph	4-CF₃-CH₂Ph	463 ± 38
(*Rac*)-6m	1	O	4-F-3-CF₃-Ph	2,4-diCl-CH₂Ph	630 ± 25
(*Rac*)-6n	0	-	4-F-3-CF₃-Ph	Ph	65 ± 13
(*Rac*)-6o	0	-	4-F-3-CF₃-Ph	2-CH₃CH₂-6-CH₃Ph	635 ± 18
(*Rac*)-6p	0	-	4-F-3-CF₃-Ph	4,6-(OCH₃)₂-pyrimidin-2-yl	200 ± 20
(*Rac*)-6q	0	-	4-F-3-CF₃-Ph	1*H*-1,2,4-triazol-3-yl	242 ± 13
(*Rac*)-6r	1	CH₂	1-Me-3-CF₃-1*H*-pyrazol-5-yl	Ph	72 ± 14
(*Rac*)-6s	1	CH₂	2-CF₃-pyridin-4-yl	Ph	188 ± 14
(*Rac*)-6t	1	CH₂	6-Cl-3-phenypyridazin-4-yl	Ph	555 ± 25
(*Rac*)-6u	1	CH₂	3-Cl-5-CF₃-pyridin-2-Ph-4-yl	Ph	328 ± 28
(*Rac*)-6v	1	CH₂	4'-F-3'-CF₃- [1,1'-biphenyl]-4-yl	Ph	332 ± 31
(*S*)-6a	1	CH₂	4-F-3-CF₃-Ph	pyrimidin-2-yl	105 ± 25
(*S*)-6h	1	CH₂	4-F-3-CF₃-Ph	CH(CH₂)₅	44 ± 13
(*S*)-6n	0	-	4-F-3-CF₃-Ph	Ph	28 ± 4
(*S*)-6q	0	-	4-F-3-CF₃-Ph	1*H*-1,2,4-triazol-3-yl	138 ± 38
(S)-BF	1	CH₂	4-F-3-CF₃-Ph	Ph	8 ± 2
(*Rac*)-BF	1	CH₂	4-F-3-CF₃-Ph	Ph	32 ± 3
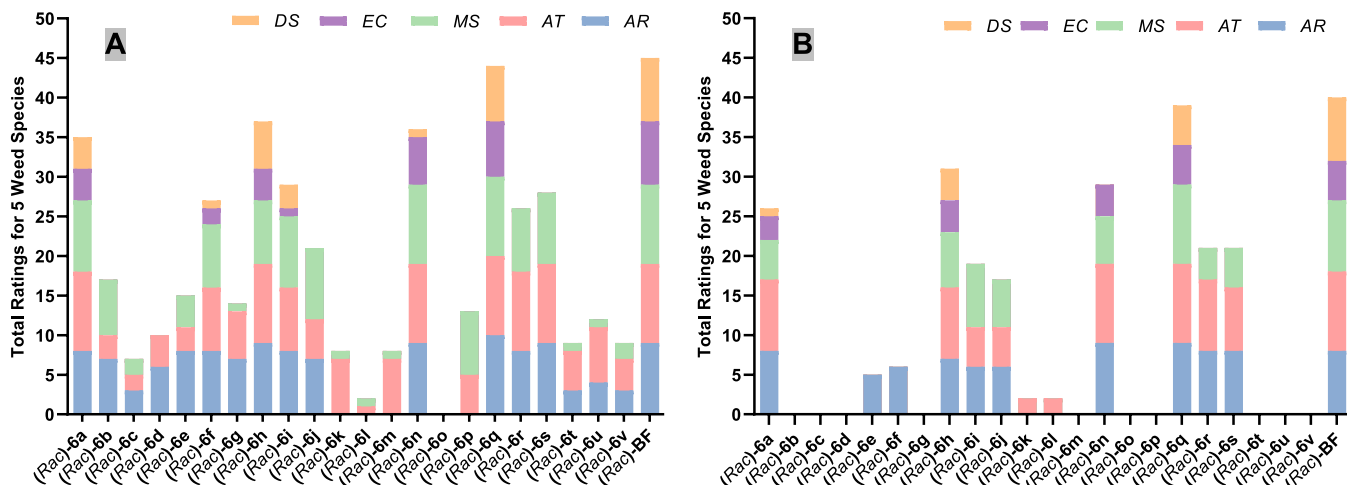
[a]PDS inhibitory activity (U/L) at 3 days post-application.

with a column temperature maintained at 30 °C. The sample size injected was 2 μL. The mobile phase consisted of A: 0.1% formic acid water and B: methanol. The flow rate was set at 0.5 mL/min, and the mobile phase elution program followed A: 90% and B: 10%.
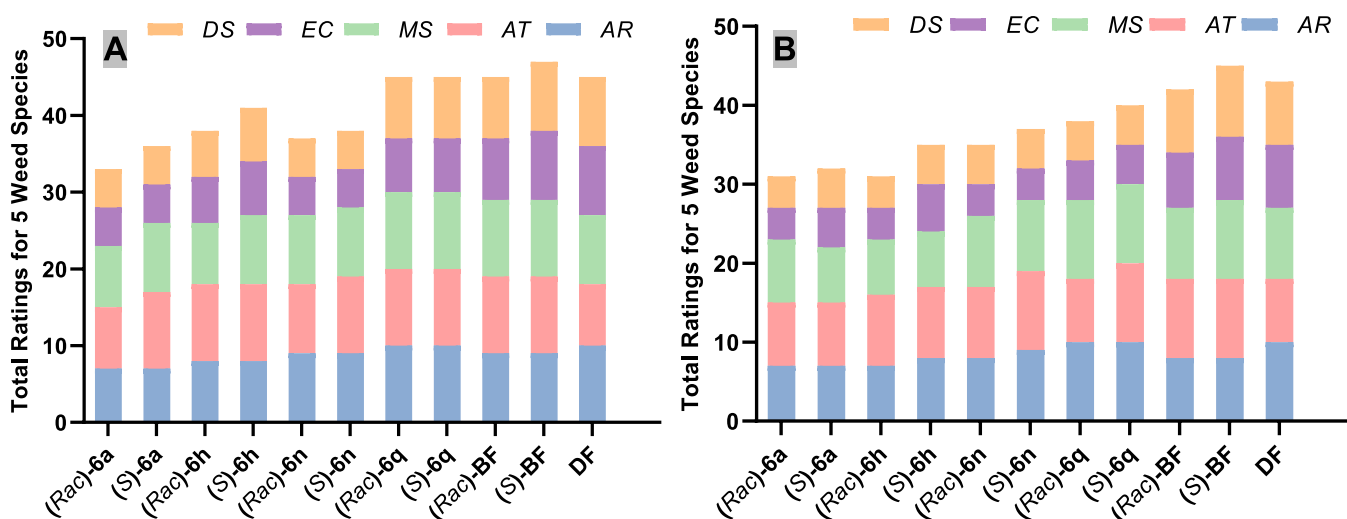
Mass Spectrum Conditions. The atmospheric pressure electrospray ion source (ESI+) was utilized in multiple reaction detection modes (MRM), the qualitative ion pair was 356.2/91.1, and the

corresponding collision energy was 48.5 eV. The quantitative ion pair was 356.2/162.1, and the corresponding collision energy was 34.3 eV.

Linear Regression Equation. Dilute the standard solution with methanol to prepare 0.005, 0.01, 0.1, 0.2, 1, and 2 mg/L series standard solutions. Take the (*S*)-BF injection concentration (x, mg/L) as the abscissa and the chromatographic peak area (y) of quantitative ions as the ordinate for the linear regression calculation.

Figure 3. Postemergent herbicidal activity of compound **6**. (A) Dosage 300 g ai/ha. (B) Dosage 150 g ai/ha. Each value represents the mean of three experiments. Abbreviations: *AR*, *Amaranthus retroflexus*; *AT*, *Abutilon theophrasti*; *MS*, *Medicago sativa*; *EC*, *Echinochloa crus-galli*; and *DS*, *Digitaria sanguinalis*. Rating scale of inhibition percent in relation to the untreated control: 10, 100%; 9, 90−99%; 8, 80−89%; 7, 70−79%; 6, 60−69%; 5, 50−59%; 4, 40−49%; 3, 30−39%; 2, 20−29%; 1, 10−19%; and 0, 0−9%.

Figure 4. Postemergent herbicidal activity of compounds (*Rac*)-**6a**, (*S*)-**6a**, (*Rac*)-**6h**, (*S*)-**6h**, (*Rac*)-**6n**, (*S*)-**6n**, (*Rac*)-**6q**, and (*S*)-**6q**. (A) Dosage 300 g ai/ha. (B) Dosage 150 g ai/ha. Each value represents the mean of three experiments. Abbreviations: *AR*, *Amaranthus retroflexus*; *AT*, *Abutilon theophrasti*; *MS*, *Medicago sativa*; *EC*, *Echinochloa crus-galli*; and *DS*, *Digitaria sanguinalis*. Rating scale of inhibition percent in relation to the untreated control: 10, 100%; 9, 90−99%; 8, 80−89%; 7, 70−79%; 6, 60−69%; 5, 50−59%; 4, 40−49%; 3, 30−39%; 2, 20−29%; 1, 10−19%; and 0, 0−9%.

The linear equation was $y = 6000000x + 261830$, and R^2 was 0.9963 (Figure S2).

RESULTS AND DISCUSSION

Synthesis. According to Scheme 1, (*Rac*)-BF, (*S*)-BF, and the (*Rac*)-**6** compounds were synthesized with yields of 61−80%. (*Rac*)-BF, (*S*)-BF, and compound (*Rac*)-**6n** were known compounds, and our ^{1}H NMR and ^{13}C NMR data were consistent with those reported in the literature.

As shown in Scheme 1, compound **1** was substituted with ethyl 2-bromobutyrate in an acetone solution containing potassium carbonate and was reflux reacted for 10 h to obtain compound **2**. The ester (compound **2**) was hydrolyzed with lithium hydroxide to form the corresponding acid (compound **3**) at room temperature with methanol and water. Compound **3** reacted with oxalyl chloride in a DCM solution, which was catalyzed by DMF and reacted at room temperature for 2 h to

obtain acyl chloride (compound **3**). Compound **3** reacted with compound **5** in a DCM solution of triethylamine to obtain the target compound **6** with a total yield of 61−80% in four steps.

For the synthesis of chiral compounds, (*R*)-2-aminobutyric acid and NaNO$_2$ in 48% HBr aqueous solution were reacted to obtain (*R*)-2-bromobutyric acid. (*R*)-2-Bromobutanoic acid was esterified with ethanol to obtain ethyl (*R*)-2-bromobutanoate. Chiral target compounds (*S*)-**6a**, (*S*)-**6h**, (*S*)-**6n**, and (*S*)-**6q** were then synthesized with (*R*)-2-bromobutanoate through the same method as illustrated in the synthesis of racemic compounds **6**. Chiral compounds (*S*)-BF, (*S*)-**6a**, (*S*)-**6h**, (*S*)-**6n**, and (*S*)-**6q** were obtained in moderate to good yields and er values (67% yield, 91:9 er; 63% yield, 88:12 er; 63% yield, 88:12 er; 61% yield, 87:13 er; 69% yield, 87:13 er; 66% yield, 85:15 er), and detailed experimental data is shown in the Supporting Information.

Figure 5. Postemergent herbicidal activity of compounds (*S*)-**6h** and (*S*)-**6q** (300 g ai/ha, 14 days after spraying). (A) *Amaranthus retroflexus* (*AR*). (B) *Abutilon theophrasti* (*AT*). (C) *Medicago sativa* (*MS*).

Herbicidal Activity, PDS Inhibitory Activity, and Structure−Activity Relationship. Takematsu et al. investigated the herbicidal activity of *N*-benzyl-2-(4-fluoro-3-trifluoromethyl phenoxy) butanoic amide and discovered the herbicide (*Rac*)-BF.[32] Since the SAR was not reported in the patent, we used a series of (*Rac*)-BF analogues for SAR analysis of phenoxamide herbicides in the search for more active compounds.

To investigate the SAR of phenoxamide herbicides, four series of compounds were designed, and their herbicidal activity was tested at dosages of 150 and 300 g ai/ha for SAR analysis. Series **I** comprised compounds (*Rac*)-**6a** to (*Rac*)-**6h**; series **II** comprised compounds (*Rac*)-**6i** to (*Rac*)-**6m**; series **III** comprised compounds (*Rac*)-**6n** to (*Rac*)-**6q**; and series **IV** comprised compounds (*Rac*)-**6r** to (*Rac*)-**6v**. The experimental results showed (Figure 3 and Table S1) that compounds (*Rac*)-**6a**, (*Rac*)-**6f**, (*Rac*)-**6h**, (*Rac*)-**6i**, (*Rac*)-**6n**, (*Rac*)-**6q**, (*Rac*)-**6r**, and (*Rac*)-**6s** exhibited effective control of *AR*, *AT*, and *MS* broadleaf weeds (inhibition rates were all higher than 80%). These compounds displayed activity comparable to that of the positive control agent (*Rac*)-BF. Compound (*Rac*)-**6n** has been reported to have excellent herbicidal activity by patients, and the results of this experiment were the same.[33] Additionally, compounds (*Rac*)-**6a**, (*Rac*)-**6h**, (*Rac*)-**6n**, and (*Rac*)-**6q** demonstrated certain herbicidal activities against *EC* and *DS* weeds (inhibition rates of 10−70%). Notably, compound (*Rac*)-**6q** exhibited the same activity as the positive control agent (*Rac*)-BF. To further investigate the herbicidal activity of the target compounds, the application concentration was reduced to 150 g ai/ha. The results revealed that compounds (*Rac*)-**6a**, (*Rac*)-**6h**, (*Rac*)-**6n**, and (*Rac*)-**6q** displayed higher herbicidal activity against all five weed species compared to those of the other compounds in the study.

According to the literature, it has been reported that the *S* configuration of BF exhibits herbicidal activity that is 1000 times higher than that of the *R* configuration.[10,11] Therefore, we synthesized the chiral structure of compounds (*S*)-**6a**, (*S*)-**6h**, (*S*)-**6n**, and (*S*)-**6q** and evaluated their herbicidal activity against five weed species at dosages of 300 and 150 g ai/ha (Figures 3, 4, and 5 and Tables S1 and S2). The results showed that compounds (*S*)-**6a**, (*S*)-**6h**, (*S*)-**6n**, and (*S*)-**6q** exhibited excellent herbicidal activity against all five weed species, which was higher than for their racemic mixtures. These compounds have shown potential as lead candidates for the development of herbicides. Unfortunately, at 75 g ai/ha, the herbicidal activity of these compounds decreased significantly (Table S3).

Consequently, we wanted to determine whether the benzene ring at R[2] can be replaced by other aromatic rings. As shown in Figures 3 and 4 and Tables S1 and S2, when *n* = 1 and X was CH₂, we synthesized compounds (*Rac*)-**6a** (pyrimidine), (*Rac*)-**6b** (biphenyl), (*Rac*)-**6c**, (*Rac*)-**6d** (phenoxyphen), (*Rac*)-**6e** (benzo[*d*][1,3]dioxole), (*Rac*)-**6f** (pyrazin), and

(*Rac*)-**6g** (naphthalene). The results showed that the hierarchy of the herbicidal activity was Ph > pyrimidine > pyrazin > biphenyl > benzo[*d*][1][1]dioxole > naphthalene > phenoxyphen > 4-CN-Ph. SAR analysis showed that R² was unfavorable for aryl and other substituted phenyls with large hindrances. When the R² was cyclohexane ((*Rac*)-**6h**), the herbicidal activity was slightly lower than that of phenyl ((*Rac*)-BF).

Next, based on the theoretical design of bioisosterism, compounds (*Rac*)-**6i** to (*Rac*)-**6m** were synthesized by replacing methylene with an oxygen atom. The experimental results showed that the herbicidal symptoms of compounds (*Rac*)-**6i** to (*Rac*)-**6m** were similar to those of hormonal herbicides, both of which would cause swelling of stems and contraction of leaves. Further studies were needed to determine whether this was a hormonal herbicide. The results of herbicidal activity showed that the herbicidal activity was the highest when there were no substituents at the benzyl.

We further investigated the effects of the X group on the herbicidal structure. Compounds (*Rac*)-**6n** to (*Rac*)-**6q** were synthesized. The compound (*Rac*)-**6q** exhibited excellent herbicidal activity, which was equivalent to that of the commercial herbicide BF.

To enhance the SAR of (*Rac*)-BF, we investigated the SAR of the R¹ position. As part of this study, compounds (*Rac*)-**6r** to (*Rac*)-**6v** were synthesized. The results showed that compounds (*Rac*)-**6r** and (*Rac*)-**6s** exhibited effective control against broadleaf weeds but had no impact on grass weeds. SAR analysis revealed that the most active group at the R¹ position was 4-F-3-CF₃-Ph. It was observed that moderate herbicidal activity was observed in the leaves when R¹ was substituted with pyridinyl ((*Rac*)-**6s**) and substituted for pyrazole ((*Rac*)-**6r**).
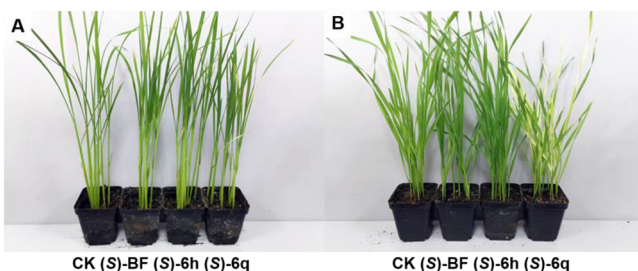
To further demonstrate that the synthesized BF analogues functioned as PDS inhibitors, an *in vivo* assessment of PDS inhibitory activity was conducted for all of the target compounds. As illustrated in Scheme 1, compounds **6a**, **6h**, **6n**, and BF, which exhibited high herbicidal activities, showed low concentrations of enzyme activities. This phenomenon clearly supports that compounds **6a**, **6h**, and **6n** act as PDS inhibitors. However, compound **6q** showed both high herbicidal activity and a high PDS activity concentration. We assume that compound **6q** might act through an alternative mechanism, through the inhibition of cytochrome synthesis, to exhibit excellent herbicidal activities.

Crop Selectivity. To evaluate the postemergence crop safety of compounds (*Rac*)-**6h**, (*S*)-**6h**, (*Rac*)-**6q**, and (*S*)-**6q**, we conducted tests on six representative crops, namely, wheat, rice, peanut, maize, soybeans, and cotton. The results presented in Table 1 and Figure 6 demonstrate that compounds (*Rac*)-BF, (*S*)-BF, (*Rac*)-**6q**, and (*S*)-**6q** exhibit high sensitivity to peanuts, soybeans, and cotton at a dosage of

Table 1. Postemergent Crop Selectivity of Compounds (Rac)-6h, (S)-6h, (Rac)-6q, and (S)-6q (300 g ai/ha)

compounds	wheat	rice	peanut	maize	soybeans	cotton
(Rac)-6h	0[a]	0	2	1	5	3
(S)-6h	0	0	3	2	5	3
(Rac)-6q	8	6	4	2	7	6
(S)-6q	8	6	4	2	7	6
(Rac)-BF	0	1	5	4	10	10
(S)-BF	0	1	6	5	10	10

[a]Rating scale of inhibition percent in relation to the untreated control: 10, 100%; 9, 90−99%; 8, 80−89%; 7, 70−79%; 6, 60−69%; 5, 50−59%; 4, 40−49%; 3, 30−39%; 2, 20−29%; 1, 10−19%; and 0, 0−9%.
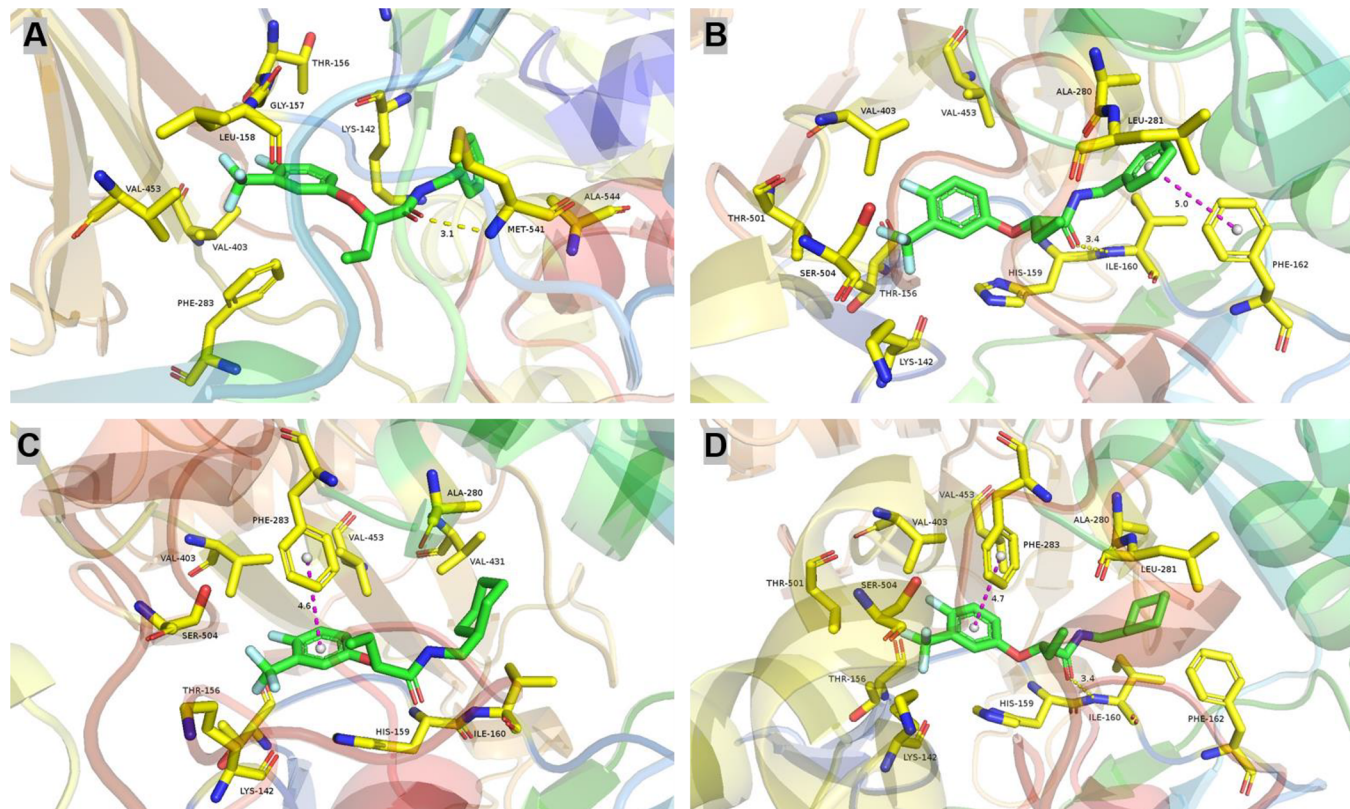
Figure 6. Postemergent crop selectivity of compounds (S)-6h and (S)-6q (300 g ai/ha). (A) Rice. (B) Wheat.

300 g ai/ha. Upon initial application, varying degrees of bleaching symptoms were observed in both leaves and stems. However, the selectivity of compounds (Rac)-6h and (S)-6h was significantly superior to that of the aforementioned compounds. (Rac)-BF and (S)-BF also displayed high sensitivity toward peanuts and maize, causing the albinism of leaves and stems in the early stages of application. Although crop growth could recover in later stages, it was affected during that period. Conversely, the sensitivity of compound (Rac)-6h toward maize was significantly lower than that of (Rac)-BF and (S)-BF. While a slight albinism of leaves was observed in the early stages of application, the injury could be overcome in the later stages of growth without a significant impact on overall crop growth. Compounds (Rac)-6q and (S)-6q showed high sensitivity toward wheat and rice. Three days after application, the stems of wheat and rice began to show albinism, resulting in severe chemical injury. It was initially speculated that compounds (Rac)-6q and (S)-6q contained triazole functional groups, which had strong internal absorption, and wheat roots were multicut and developed, which were important causes of pesticide injury.[34,35] At the same time, compounds (Rac)-BF, (S)-BF, (Rac)-6h, and (S)-6h did not injure wheat, which also verified that (Rac)-BF and (S)-BF were mainly used for weeding wheat fields.[3] Therefore, compounds (Rac)-BF, (Rac)-6h, and (Rac)-6q had higher selectivity than the S configuration for six crops. Compounds (Rac)-6h and (S)-6h can be used as candidate pesticides to control broadleaf weeds in wheat, rice, maize, and peanut fields. Compounds (Rac)-6q and (S)-6q can be used as candidate pesticides for the control of broadleaf weeds in maize fields.

Molecular Docking. To explain the superiority of active compound S configuration over R configuration, compounds (R)-BF, (S)-BF, (R)-6h, and (S)-6h were selected for molecular docking with OsPDS, and the binding conforma-

Figure 7. Molecular docking of compounds (R)-BF, (S)-BF, (R)-6h, and (S)-6h with OsPDS. (A) 3D interaction diagram of (R)-BF. (B) 3D interaction diagram of (S)-BF. (C) 3D interaction diagram of compound (R)-6h. (D) 3D interaction diagram of compound (S)-6h.

I

tions of each compound were compared. As can be seen from Figure 7 and Figure S4, hydrogen bonds, halogen (fluorine), alkyl, and π-alkyl were among the binding modes of the four compounds with *Os*PDS. It was found that the binding modes of compounds (*S*)-BF and (*S*)-**6h** with *Os*PDS were higher than those of compounds (*R*)-BF and (*R*)-**6h**. The fluorine atom of trifluoromethyl on (*S*)-BF formed two hydrogen bonds of 3.33 and 3.13 Å with Thr501 and Ser504, and the carbonyl group formed two hydrogen bonds of 3.40 and 3.36 Å with Ile160 and His159. The fluorine atom of trifluoromethyl on compound (*S*)-**6h** formed two hydrogen bonds of 3.34 and 3.14 Å with Thr501 and Ser504, and the carbonyl group position formed two hydrogen bonds of 3.36 and 3.26 Å with Ile160 and His159. At the same time, (*S*)-BF has a $\pi-\pi$ stacking interaction with Phe162 and an amide-π stacking interaction with Ala280 at the right benzene ring position. The cyclohexane site on the upper right of compound (*S*)-**6h** forms a π-alkyl stacking interaction with Phe162. However, the fluorine atom of trifluoromethyl on (*R*)-BF forms a 2.38 Å hydrogen bonding interaction with Leu158, and the carbonyl position forms a 2.70 Å hydrogen bonding interaction with Met541. The fluorine atom of trifluoromethyl on compound (*R*)-**6h** formed a 3.21 Å hydrogen bonding interaction with Ser504, and the carbonyl group position formed a 3.34 Å hydrogen bonding interaction with His159. The benzene ring to the left of compound (*R*)-**6h** forms a $\pi-\pi$ stacking interaction with Phe283. Based on the influence of compounds (*Rac*)-BF and (*Rac*)-**6h**, the *R/S* configuration ethyl deviates in different directions. The *S* configuration has more interactions with the residues in the active pocket than does the *R* configuration, which improves the binding affinity with *Os*PDS and has higher herbicidal activity. The binding energies of compounds (*R*)-BF, (*S*)-BF, (*R*)-**6h**, and (*S*)-**6h** to *Os*PDS were −9.2, −9.7, −9.3, and −9.7 kcal/mol, respectively.

Digestion Dynamics of (*S*)-BF in Wheat Plants. According to Table S4, the recovery of (*S*)-BF in plants was 95.08−97.82%, and the RSD was 0.68−2.24%, which meets the requirements of residue determination.
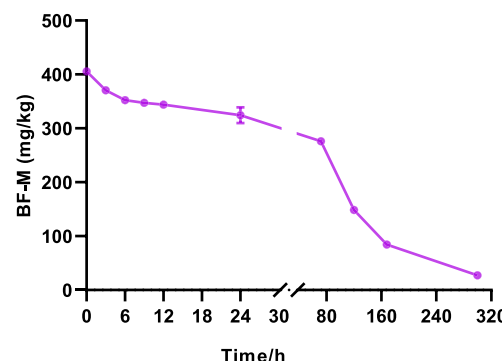
As shown in Figure 1, Buerge et al. reported that the herbicide (*S*)-BF was found to form two metabolites in plants, animals, and soil: phenoxybutanamide (a minor metabolite, BF-amide) and phenoxybutanoic acid (a major metabolite, BF-acid).[10,11] Since compounds (*Rac*)-**6h**, (*S*)-**6h**, (*Rac*)-**6q**, and (*S*)-**6q** were similar in structure to (*Rac*)-BF and (*S*)-BF, the production of the same BF-amide and BF-acid metabolites had similar digestive kinetics in plants. Therefore, only (*S*)-BF was evaluated to represent the digestion dynamics of these compounds in wheat when measuring the digestion dynamics of the compounds in wheat.

As shown in Table 2 and Figure 8, the degradation rate of (*S*)-BF in wheat was relatively slow within the first 12 h, and the degradation rate of (*S*)-BF in wheat increased after 12 h and became stable at 300 h. There was no significant difference among the three treatment periods of 6, 9, and 12 h. In addition, there was a significant difference after each treatment period time. As can be seen from Table S5, the degradation half-life of (*S*)-BF in wheat was 77.02 h, with the resolution equation being $C_t = 399.64e^{-0.009t}$ and R^2 being 0.9663. Therefore, the half-life of the chiral phenoxyamide herbicide represented by (*S*)-BF in wheat plants was about 3 days, and the residual amount of (*S*)-BF in wheat was very low after 14 days, which was relatively safe for crops.

Table 2. Degradation Dynamics of (*S*)-BF in Wheat Plants (*n* = 3)

time/h	(*S*)-BF (mg/kg)	RSD/%
0	405.64[a]^a	4.41
3	370.64[b]	6.01
6	352.31[c]	2.89
9	347.30[c]	1.67
12	343.97[c]	5.77
24	324.53[d]	14.56
72	276.19[e]	5.85
120	148.69[f]	1.51
168	84.19[g]	2.17
300	27.47[h]	1.67

^{a}Values sharing the different letters differ significantly (*P* < 0.05). Each value represents the average of three replicates.

Figure 8. Degradation dynamics of (*S*)-BF in wheat plants.

In summary, it was found that the structure of the phenoxyamide herbicide was closely related to the steric hindrance and electability of the substituents. The best herbicidal activity was achieved when the steric hindrance of R^1 and R^2 was small and electrically neutral. Under the conditions of 150 and 300 g ai/ha, compounds (*Rac*)-**6h** and (*Rac*)-**6q** had higher herbicidal activities against five kinds of weeds, which was equivalent to that of commercial herbicide BF. Chiral compounds (*S*)-**6h** and (*S*)-**6q** had higher herbicidal activities than compounds (*Rac*)-**6h** and (*Rac*)-**6q**. The *in vivo* inhibitory activity of PDS showed that compound **6h** was a PDS inhibitor. Molecular docking results showed that, compared with the *R* configuration, the *S* configuration had more interactions with residues in active pockets, improved binding affinity with *Os*PDS, and higher herbicidal activity. At the same time, (*S*)-BF was used to determine the digestion dynamics of phenoxyamide herbicides in wheat. The results indicate that the half-life of phenoxyamide herbicides was about 3 days. Therefore, compounds (*S*)-**6h** and (*S*)-**6q** are potential candidate lead compounds for the development of more active herbicides.

■ ASSOCIATED CONTENT

Ⓢ Supporting Information

The Supporting Information is available free of charge at https://pubs.acs.org/doi/10.1021/acs.jafc.3c04733.

Postemergent herbicidal activity of compound **6**; postemergent herbicidal activity of compounds (*Rac*)-**6a**, (*S*)-**6a**, (*Rac*)-**6h**, (*S*)-**6h**, (*Rac*)-**6n**, (*S*)-**6n**, (*Rac*)-**6q**, and (*S*)-**6q**; relationship between SAR and herbicidal activity of compound **6**; calibration curves

of (*S*)-BF 0.005−2 mg/L in the nutrient solution; sample treatment; accuracy of the method; average recovery of (*S*)-BF in wheat plants; degradation half-life of (*S*)-BF in wheat plants; molecular docking of compounds (*R*)-BF, (*S*)-BF, (*R*)-**6h**, and (*S*)-**6h** with *Os*PDS; experimental procedures for the synthesis of compounds (*Rac*)-**1u** and (*Rac*)-**1v**; HPLC spectra; and ^{1}H, ^{13}C, and ^{19}F NMR spectra for the target compounds (PDF)

AUTHOR INFORMATION

Corresponding Authors

Zhichao Jin − *National Key Laboratory of Green Pesticide, Key Laboratory of Green Pesticide and Agricultural Bioengineering, Ministry of Education, Guizhou University, Huaxi District, Guiyang 550025, People's Republic of China;* orcid.org/0000-0003-3003-6437; Email: zcjin@gzu.edu.cn

Yonggui Robin Chi − *National Key Laboratory of Green Pesticide, Key Laboratory of Green Pesticide and Agricultural Bioengineering, Ministry of Education, Guizhou University, Huaxi District, Guiyang 550025, People's Republic of China; School of Chemistry, Chemical Engineering, and Biotechnology, Nanyang Technological University, Singapore 637371, Singapore;* orcid.org/0000-0003-0573-257X; Email: robinchi@ntu.edu.sg

Authors

Meng Zhang − *National Key Laboratory of Green Pesticide, Key Laboratory of Green Pesticide and Agricultural Bioengineering, Ministry of Education, Guizhou University, Huaxi District, Guiyang 550025, People's Republic of China*

Hui Cai − *National Key Laboratory of Green Pesticide, Key Laboratory of Green Pesticide and Agricultural Bioengineering, Ministry of Education, Guizhou University, Huaxi District, Guiyang 550025, People's Republic of China*

Dan Ling − *National Key Laboratory of Green Pesticide, Key Laboratory of Green Pesticide and Agricultural Bioengineering, Ministry of Education, Guizhou University, Huaxi District, Guiyang 550025, People's Republic of China*

Chen Pang − *National Key Laboratory of Green Pesticide, Key Laboratory of Green Pesticide and Agricultural Bioengineering, Ministry of Education, Guizhou University, Huaxi District, Guiyang 550025, People's Republic of China*

Jinming Chang − *National Key Laboratory of Green Pesticide, Key Laboratory of Green Pesticide and Agricultural Bioengineering, Ministry of Education, Guizhou University, Huaxi District, Guiyang 550025, People's Republic of China*

Complete contact information is available at:
https://pubs.acs.org/10.1021/acs.jafc.3c04733

Notes
The authors declare no competing financial interest.

ACKNOWLEDGMENTS

REFERENCES

(1) http://www.stats.gov.cn/sj/zxfb/202302/t20230228_1919011.html.

(2) Liu, H. Y.; Yu, L. K.; Qin, S. N.; Yang, H. Z.; Wang, D. W.; Xi, Z. Design, synthesis, and metabolism studies of *N*-1,4-diketophenyltriazinones as protoporphyrinogen IX oxidase inhibitors. *J. Agric. Food Chem.* **2023**, *71*, 3225−3238.

(3) Yang, L. J.; Wang, D. W.; Ma, D. J.; Zhang, D.; Zhou, N.; Wang, J.; Xu, H.; Xi, Z. In silico structure-guided optimization and molecular simulation studies of 3-phenoxy-4-(3-trifluoromethylphenyl) pyridazines as potent phytoene desaturase inhibitors. *Molecules* **2021**, *26*, 6979.

(4) Li, J. H.; Wang, Y.; Wu, Y. P.; Li, R. H.; Liang, S.; Zhang, J.; Zhu, Y. G.; Xie, B. J. Synthesis, herbicidal activity study and molecular docking of novel pyrimidine thiourea. *Pestic. Biochem. Phys.* **2021**, *172*, No. 104766.

(5) Fang, J.; He, Z.; Liu, T.; Li, J.; Dong, L. A novel mutation Asp-2078-Glu in ACCase confers resistance to ACCase herbicides in barnyardgrass (*Echinochloa crus-galli*). *Pestic. Biochem. Phys.* **2020**, *168*, No. 104634.

(6) Lu, H.; Yu, Q.; Han, H.; Owen, M. J.; Powles, S. B. Evolution of resistance to HPPD-inhibiting herbicides in a wild radish population via enhanced herbicide metabolism. *Pest Manag. Sci.* **2020**, *76*, 1929−1937.

(7) Peterson, M. A.; Collavo, A.; Ovejero, R.; Shivrain, V.; Walsh, M. J. The challenge of herbicide resistance around the world: a current summary. *Pest Manag. Sci.* **2018**, *74*, 2246−2259.

(8) Liu, Y. C.; Qu, R. Y.; Chen, Q.; Yang, J. F.; Niu, C. W.; Zhen, X.; Yang, G. F. Triazolopyrimidines as a new herbicidal lead for combating weed resistance associated with acetohydroxyacid synthase mutation. *J. Agric. Food Chem.* **2016**, *64*, 4845−4857.

(9) Liu, X. H.; Xu, X. Y.; Tan, C. X.; Weng, J. Q.; Xin, J. H.; Chen, J. Synthesis, crystal structure, herbicidal activities and 3D-QSAR study of some novel 1,2,4-triazolo[4,3-a]pyridine derivatives. *Pest Manag. Sci.* **2015**, *71*, 292−301.

(10) Buerge, I. J.; Müller, M. D.; Poiger, T. The chiral herbicide beflubutamid (II): enantioselective degradation and dnantiomerization in soil, and formation/degradation of chiral metabolites. *Environ. Sci. Technol.* **2013**, *47*, 6812−6818.

(11) Buerge, I. J.; Bachli, A.; De Joffrey, J. P.; Muller, M. D.; Spycher, S.; Poiger, T. The chiral herbicide beflubutamid (I): Isolation of pure enantiomers by HPLC, herbicidal activity of enantiomers, and analysis by enantioselective GC-MS. *Environ. Sci. Technol.* **2013**, *47*, 6806−6811.

(12) Zhang, Y.; Zhou, L.; Li, R.; Li, Y.; Tan, Y.; Shi, H.; Wang, M. Comprehensive assessment of enantioselective bioactivity, toxicity, and dissipation in soil of the chiral herbicide flurtamone. *J. Agric. Food Chem.* **2023**, *71*, 4810−4816.

(13) Qin, G.; Gu, H.; Ma, L.; Peng, Y.; Deng, X. W.; Chen, Z.; Qu, L. J. Disruption of phytoene desaturase gene results in albino and dwarf phenotypes in arabidopsis by impairing chlorophyll, carotenoid, and gibberellin biosynthesis. *Cell Res.* **2007**, *17*, 471−482.

(14) Lu, H.; Yu, Q.; Han, H.; Owen, M. J.; Powles, S. B. Non-target-site resistance to PDS-inhibiting herbicides in a wild radish (raphanus raphanistrum) population. *Pest Manag. Sci.* **2020**, *76*, 2015−2020.

(15) Wang, Y.; Li, M.; Chen, J.; Tao, Y.; Wang, X. O-to-S substitution enables dovetailing conflicting cyclizability, polymerizability, and recyclability: dithiolactone vs. dilactone. *Angew. Chem., Int. Ed.* **2021**, *60*, 22547−22553.

(16) Datar, R. V.; Mao, J. H. A method for synthesizing *S*-beflubufamid from (*R*)-2-aminobutyric acid. CN Patent CN115087633A, Sept 20, 2022.

(17) Tang, J. Y.; Jiang, B. F. The invention relates to a preparation method of *α*-bromo-fatty acid ester. CN Patent CN109503354A, Mar 22, 2019.

(18) Zhang, C.; Wu, X.; Li, Y.; Liang, C.; Che, Y.; Gu, L.; Ren, J.; Hu, K.; Sun, X.; Yang, C.-H.; Chen, X. Synthesis and bioactivity of novel inhibitors for type III secretion system of pseudomonas aeruginosa PAO1. *Chin. J. Org. Chem.* **2013**, *33*, 1309−1318.

(19) Zhang, W. D. The invention relates to a synthesis method of beflubufamid. CN Patent CN102766067A, Nov 7, 2012.

(20) Endean, R. T.; Rasu, L.; Bergens, S. H. Enantioselective hydrogenations of esters with dynamic kinetic resolution. *ACS Catal.* **2019**, *9*, 6111−6117.

(21) Song, J. L.; Chen, S. Y.; Xiao, L.; Xie, X. L.; Zheng, Y. C.; Zhang, S. S.; Shu, B. Rh(III)-catalyzed *N*-arylation of alkyl dioxazolones with arylboronic acids for the synthesis of *N*-aryl amides. *Eur. J. Org. Chem.* **2022**, *2022*, No. e202200710.

(22) Cheshmazar, N.; Hemmati, S.; Hamzeh-Mivehroud, M.; Sokouti, B.; Zessin, M.; Schutkowski, M.; Sippl, W.; Nozad Charoudeh, H.; Dastmalchi, S. Development of new inhibitors of HDAC1−3 enzymes aided by in silico design strategies. *J. Chem. Inf. Model* **2022**, *62*, 2387−2397.

(23) Wu, L.; Hao, Y.; Liu, Y.; Wang, Q. NIS-mediated oxidative arene C(sp^2)-H amidation toward 3,4-dihydro-2(*1H*)-quinolinone, phenanthridone, and *N*-fused spirolactam derivatives. *Org. Biomol. Chem.* **2019**, *17*, 6762−6770.

(24) Hanada, S.; Tsutsumi, E.; Motoyama, Y.; Nagashima, H. Practical access to amines by platinum-catalyzed reduction of carboxamides with hydrosilanes: synergy of dual Si-H groups leads to high efficiency and selectivity. *J. Am. Chem. Soc.* **2009**, *131*, 15032−15040.

(25) Nan, J. X.; Dong, J.; Cao, J. Q.; Huang, G. Y.; Shi, X. X.; Wei, X. F.; Chen, Q.; Lin, H. Y.; Yang, G. F. Structure-based design of 4-hydroxyphenylpyruvate dioxygenase inhibitor as a potential herbicide for cotton fields. *J. Agric. Food Chem.* **2023**, *71*, 5783−5795.

(26) Zuo, Y.; Wu, Q.; Su, S. W.; Niu, C. W.; Xi, Z.; Yang, G. F. Synthesis, herbicidal activity, and QSAR of novel N-benzothiazolyl-pyrimidine-2,4-diones as protoporphyrinogen oxidase inhibitors. *J. Agric. Food Chem.* **2016**, *64*, 552−562.

(27) Wang, D. W.; Zhang, R. B.; Yu, S. Y.; Liang, L.; Ismail, I.; Li, Y. H.; Xu, H.; Wen, X.; Xi, Z. Discovery of novel *N*-isoxazolinylphenyl-triazinones as promising protoporphyrinogen IX oxidase inhibitors. *J. Agric. Food Chem.* **2019**, *67*, 12382−12392.

(28) Zhang, D.; Zhou, N.; Yang, L. J.; Yu, Z. L.; Ma, D. J.; Wang, D. W.; Li, Y. H.; Liu, B.; Wang, B. F.; Xu, H.; Xi, Z. Discovery of (5-(benzylthio)-4-(3-(trifluoromethyl)phenyl)-4H-1,2,4-triazol-3-yl) methanols as potent phytoene desaturase inhibitors through virtual screening and structure optimization. *J. Agric. Food Chem.* **2022**, *70*, 10144−10157.

(29) Zhou, Y.; Yu, Y.; Huang, Q.; Zheng, H.; Zhan, R.; Chen, L.; Meng, X. Simultaneous determination of 26 pesticide residues in traditional Chinese medicinal leeches by modified QuEChERS coupled with HPLC-MS/MS. *ACS Omega* **2023**, *8*, 12404−12410.

(30) Zhang, M.; Dou, M.; Xia, Y.; Hu, Z.; Zhang, B.; Bai, Y.; Xie, J.; Liu, Q.; Xie, C.; Lu, D.; Hou, S.; He, J.; Tao, J.; Sun, R. Photostable 1-trifluoromethyl cinnamyl alcohol derivatives designed as potential fungicides and bactericides. *J. Agric. Food Chem.* **2021**, *69*, 5435−5445.

(31) Liu, W.; Su, Y.; Liu, J.; Zhang, K.; Wang, X.; Chen, Y.; Duan, L.; Shi, F. Determination of cyflufenamid residues in 12 foodstuffs by QuEChERS-HPLC-MS/MS. *Food Chem.* **2021**, *362*, No. 130148.

(32) Takematsu, T.; Takeuchi, Y.; Takenaka, M.; Takamura, S.; Matsushita, A. *N*-Benzyl-2-(4-fluoro-3-trifluoromethylphenoxy) butanoic amide and herbicidal composition containing the same. EP Patent EP0239414A1, Sept 30, 1987.

(33) David, M. Anilide herbicides. EP Patent EP0289100A2, Nov 02, 1988.

(34) Liu, X.; Xu, J.; Li, Y.; Dong, F.; Li, J.; Song, W.; Zheng, Y. Rapid residue analysis of four triazolopyrimidine herbicides in soil, water, and wheat by ultra-performance liquid chromatography coupled to tandem mass spectrometry. *Anal. Bioanal. Chem.* **2011**, *399*, 2539−2547.

(35) Zhong, M.; Wang, T.; Hu, J. Dissipation kinetics and residues of triazolopyrimidine herbicides flumetsulam and florasulam in corn ecosystem. *Environ. Monit. Assess.* **2015**, *187*, 390.